

---

Doctoral Dissertations

Student Theses and Dissertations

---

1971

## Internal friction of ion exchanged $\text{Li}_2\text{O}\cdot\text{Al}_2\text{O}_3\cdot 2\text{SiO}_2$ glasses

A. Ismail A. Abdel-Latif

Follow this and additional works at: [https://scholarsmine.mst.edu/doctoral\\_dissertations](https://scholarsmine.mst.edu/doctoral_dissertations)



Part of the [Ceramic Materials Commons](#)

Department: **Materials Science and Engineering**

---

### Recommended Citation

Abdel-Latif, A. Ismail A., "Internal friction of ion exchanged  $\text{Li}_2\text{O}\cdot\text{Al}_2\text{O}_3\cdot 2\text{SiO}_2$  glasses" (1971). *Doctoral Dissertations*. 1844.

[https://scholarsmine.mst.edu/doctoral\\_dissertations/1844](https://scholarsmine.mst.edu/doctoral_dissertations/1844)

This thesis is brought to you by Scholars' Mine, a service of the Missouri S&T Library and Learning Resources. This work is protected by U. S. Copyright Law. Unauthorized use including reproduction for redistribution requires the permission of the copyright holder. For more information, please contact [scholarsmine@mst.edu](mailto:scholarsmine@mst.edu).

111

INTERNAL FRICTION OF ION EXCHANGED  
 $\text{Li}_2\text{O} \cdot \text{Al}_2\text{O}_3 \cdot 2\text{SiO}_2$  GLASSES

by

A. ISMAIL A. ABDEL-LATIF, 1944-

A DISSERTATION

Presented to the Faculty of the Graduate School of the

UNIVERSITY OF MISSOURI-ROLLA

In Partial Fulfillment of the Requirements for the Degree

DOCTOR OF PHILOSOPHY

in

CERAMIC ENGINEERING

1971

T2621  
107 pages  
c.1

Walter W. Brown  
Advisor

Robert E. Moore

Charles A. Souell

W. H. Anderson

H. O. McDonald

202905

THIS THESIS IS DEDICATED

TO

MY MOTHER AND THE MEMORY OF MY LATE FATHER

## PUBLICATION THESIS OPTION

This thesis has been prepared in the style specified by the Journal of the American Ceramic Society. Pages 1-51 were submitted for publication, in August 1971, in this journal. Appendix E, pages 73-91 , was also submitted for publication in the same journal. Appendices A, B, C and D have been added for the purposes normal to thesis writing.

## ABSTRACT

$\text{Li}_2\text{O}\cdot\text{Al}_2\text{O}_3\cdot 2\text{SiO}_2$  glass fibers were ion-exchanged from 1 to 300 minutes in a sodium nitrate bath at  $366^\circ\text{C}$ . The internal friction was measured along with the lithium and sodium concentration profiles. As sodium progressively replaced lithium, the alkali internal friction peak became smaller while a new peak (mixed alkali peak) appeared and increased in magnitude. These changes in the internal friction are similar to those that occur upon the addition of a second alkali to glasses prepared by conventional melting. The magnitude of both internal friction peaks in ion exchanged glasses was dependent on the overall glass composition. The magnitude of the alkali peak depended upon the unexchanged glass core, whereas that of the mixed alkali peak depended upon the exchanged layer on the glass surface. Dissolving the exchanged surface layer led to the restoration of the original alkali peak and the disappearance of the mixed alkali peak. Changing the alkali distribution did not affect much the mixed alkali peak, but caused the alkali peak to shift to higher temperatures and become smaller. The activation energy for both peaks remained essentially constant during ion exchange of the chilled fibers and this is attributed to the rigid network structure at  $366^\circ\text{C}$ . The height of the alkali peak can be

used to determine the maximum depth of penetration of the second alkali.

## ACKNOWLEDGEMENTS

The author wishes to thank his advisor, Dr. Delbert E. Day for his help, advice and encouragement. Appreciation is also extended to Dr. Norbert J. Kreidl for his continuous interest and valuable discussions.

Thanks are due to Messrs. N. Tibbs and Zuhair Elshaieb, at the Geology department of UMR, for their cooperation in allowing the use of the Atomic Absorption Spectrophotometer.

The financial support provided by the Army Research Office - Durham, North Carolina, from September 1969 - August 1971, is gratefully acknowledged.

## TABLE OF CONTENTS

	Page
ABSTRACT . . . . .	iv
ACKNOWLEDGEMENTS . . . . .	vi
LIST OF FIGURES . . . . .	x
LIST OF TABLES . . . . .	xv
I. INTRODUCTION . . . . .	1
(A) Single Alkali Glasses . . . . .	1
(B) Mixed Alkali Glasses . . . . .	1
(C) Ion Exchange and Internal Friction . . . . .	2
II. OBJECTIVE OF INVESTIGATION . . . . .	5
III. EXPERIMENTAL PROCEDURE . . . . .	7
(A) Sample Preparation . . . . .	7
(B) Ion Exchange . . . . .	7
(C) Internal Friction Measurements . . . . .	7
(D) Chemical Analysis . . . . .	8
IV. RESULTS . . . . .	10
(A) Change in Internal Friction With Progressive Ion-Exchange . . . . .	10
(B) Change in Internal Friction with Removal of Ion-Exchanged Layer . . . . .	14
(C) Effect of Sample Dimension on Internal Friction . . . . .	18
(D) Internal Friction of Glasses Prepared by Different Techniques . . . . .	22
(E) Effect of Alkali Ion Distribution on Internal Friction . . . . .	22



## TABLE OF CONTENTS (continued)

	Page
V. DISCUSSION . . . . .	28
(A) Change in Internal Friction with Progressive Ion Exchange . . . . .	28
(B) Change in Internal Friction with Removal of the Ion-Exchanged Layer . . . . .	30
(C) Activation Energy for Internal Friction and Interdiffusion Coefficient . . . . .	31
(D) Relation Between Alkali Peak Height and Sodium Penetration Depth . . . . .	33
(E) Effect of Sample Dimensions on Internal Friction . . . . .	36
(F) Internal Friction of Glasses Prepared by Different Techniques . . . . .	38
(G) Effect of Alkali Ion Distribution on the Internal Friction . . . . .	40
(H) Insensitivity of the Alkali Peak to Surface Compositions . . . . .	42
VI. CONCLUSIONS . . . . .	44
VII. REFERENCES . . . . .	46
VIII. APPENDICES . . . . .	52
(A) Internal Friction Measurements . . . . .	53
(B) Atomic Absorption Spectrometry . . . . .	57
(C) Effect of Alkali Ion Distribution on the Internal Friction . . . . .	62
(D) Relation Between Alkali Peak Height and Penetration Depth of Introduced Second Alkali . . . . .	65
(E) Internal Friction of Proton Exchanged $\text{Li}_2\text{O}\cdot\text{Al}_2\text{O}_3\cdot 2\text{SiO}_2$ Glass . . . . .	73

## TABLE OF CONTENTS (continued)

	Page
ABSTRACT . . . . .	74
I. INTRODUCTION . . . . .	75
II. EXPERIMENTAL . . . . .	77
III. RESULTS AND DISCUSSION . . . . .	78
IV. CONCLUSIONS . . . . .	86
REFERENCES . . . . .	87
IX. VITA . . . . .	92

## LIST OF FIGURES

Figure No.	Caption	Page
(1)	Internal friction of sodium exchanged chilled $\text{Li}_2\text{O}\cdot\text{Al}_2\text{O}_3\cdot 2\text{SiO}_2$ glass fibers after various periods of time in $\text{NaNO}_3$ bath at $366^\circ\text{C}$ ( $f = 0.5$ Hz; diameter = $350 \pm 15\mu\text{m}$ ) . . .	12
(2)	Concentration of sodium oxide in chilled $\text{Li}_2\text{O}\cdot\text{Al}_2\text{O}_3\cdot 2\text{SiO}_2$ glass fibers after various periods of time in $\text{NaNO}_3$ bath at $366^\circ\text{C}$ . . . .	13
(3)	Inverse complementary error function of Na relative concentration vs. distance from the surface. . . . .	15
(4)	Internal friction of a sodium exchanged $\text{Li}_2\text{O}\cdot\text{Al}_2\text{O}_3\cdot 2\text{SiO}_2$ glass fiber (30 minutes in $\text{NaNO}_3$ at $366^\circ\text{C}$ ) before and after removing various amounts of ion-exchanged layer ( $f = 0.41 - 0.74$ Hz; original fiber diameter = $450\mu\text{m}$ ) . . . . .	16
(5)	Concentration of sodium oxide after removing various amounts of ion-exchanged layer . . . . .	17

## LIST OF FIGURES (continued)

Figure No.	Caption	Page
(6)	Internal friction for sodium exchanged $\text{Li}_2\text{O}\cdot\text{Al}_2\text{O}_3\cdot 2\text{SiO}_2$ glass fibers, 30 minutes in $\text{NaNO}_3$ bath at $366^\circ\text{C}$ ( $f = 0.37, 0.59$ and $0.78$ Hz). . . . .	19
(7)	Concentration of sodium oxide (solid line) and lithium oxide (dashed line) in sodium exchanged $\text{Li}_2\text{O}\cdot\text{Al}_2\text{O}_3\cdot 2\text{SiO}_2$ glass fibers after 30 minutes in $\text{NaNO}_3$ bath at $366^\circ\text{C}$ . Fiber diameters = $320\mu\text{m}$ ( $\bullet$ ), $375\mu\text{m}$ (x), and $485\mu\text{m}$ (o). . . . .	20
(8)	Internal friction for sodium exchanged $\text{Li}_2\text{O}\cdot\text{Al}_2\text{O}_3\cdot 2\text{SiO}_2$ glass fiber (diameter = $370\mu\text{m}$ ) and glass bar ( $13 \times 6 \times 114$ mm) after 30 minutes in $\text{NaNO}_3$ bath at $366^\circ\text{C}$ . . . . .	21
(9)	Internal friction for a sodium exchanged (15 minutes in $\text{NaNO}_3$ at $366^\circ\text{C}$ ) and a conventionally melted fiber of same composition ( $f = 0.6$ Hz). . . . .	23
(10)	Sodium oxide concentration profiles in a sodium exchanged $\text{Li}_2\text{O}\cdot\text{Al}_2\text{O}_3\cdot 2\text{SiO}_2$ glass fiber (15 minutes in $\text{NaNO}_3$ at $366^\circ\text{C}$ ) heat treated at $590^\circ\text{C}$ before and after ion-exchange. . . . .	25

## LIST OF FIGURES (continued)

Figure No.	Caption	Page
(11)	Internal friction of sodium exchanged $\text{Li}_2\text{O}\cdot\text{Al}_2\text{O}_3\cdot 2\text{SiO}_2$ glass fiber (15 minutes in $\text{NaNO}_3$ at $366^\circ\text{C}$ ) heat treated at $590^\circ\text{C}$ before and after ion-exchange. ( $f = 0.6$ Hz). . . . .	26
(12)	Internal friction of sodium exchanged chilled $\text{Li}_2\text{O}\cdot\text{Al}_2\text{O}_3\cdot 2\text{SiO}_2$ glass fiber (5 hrs. in $\text{NaNO}_3$ at $366^\circ\text{C}$ ) before and after heat treatment at $590^\circ\text{C}$ for three hours ( $f = 0.5$ Hz). . . . .	27
(13)	Comparison of height for alkali peak and mixed alkali peak in ion exchanged (●) and conventionally melted (o) glasses . . . . .	29
(14)	Mixed alkali peak height vs. thickness of dissolved surface layer for $\text{Li}_2\text{O}\cdot\text{Al}_2\text{O}_3\cdot 2\text{SiO}_2$ glass ion-exchanged 1/2 hr. at $366^\circ\text{C}$ in $\text{NaNO}_3$ (original diameter = $450\mu\text{m}$ ). . . . .	32
(15)	Reduction in alkali peak height with sodium penetration depth . . . . .	35
(16)	Internal friction for ion exchanged and conventionally melted glasses. Solid line ( $30.6\%$ $\text{Na}_2\text{O}\cdot 2.4\%$ $\text{Li}_2\text{O}\cdot 67.0\%$ $\text{SiO}_2$ ). Dashed line	

## LIST OF FIGURES (continued)

Figure No.	Caption	Page
	(30.9%Na <sub>2</sub> O. 1.9% Li <sub>2</sub> O·67.2% SiO <sub>2</sub> ). (After H. de Waal <sup>(31)</sup> ). . . . .	39
APPENDIX A		
(1)	Diagram of inverted torsion pendulum apparatus . . . . .	54
(2)	Diagram of sonic apparatus . . . . .	56
APPENDIX C		
(1)	Internal friction of sodium exchanged chilled Li <sub>2</sub> O·Al <sub>2</sub> O <sub>3</sub> ·2SiO <sub>2</sub> glass fibers (15 minutes in NaNO <sub>3</sub> at 366°C) having different alkali ion distribution due to heat treatment at 590°C for 3 hrs. (f = 0.7 Hz). . . . .	63
APPENDIX E		
(1)	Internal friction of a Li <sub>2</sub> O·Al <sub>2</sub> O <sub>3</sub> ·2SiO <sub>2</sub> glass (chilled) before and after ion-exchange in NH <sub>4</sub> HSO <sub>4</sub> at 366°C for 21 hours (f = 0.63 Hz). . . . .	79
(2)	Infrared transmission of the specimen used for internal friction measurements, Figure 1 . Dashed curve was shifted (7%) for clarity. . . . .	80

## LIST OF FIGURES (continued)

Figure No.	Caption	Page
(3)	Internal friction of a sodium exchanged $\text{Li}_2\text{O}\cdot\text{Al}_2\text{O}_3\cdot 2\text{SiO}_2$ glass fibers (chilled) after various periods of time in $\text{NaNO}_3$ bath at $366^\circ\text{C}$ ( $f = 0.5$ Hz; diameter = $350 \pm 15\mu\text{m}$ ). . . . .	84

## LIST OF TABLES

	Page
Table I	
Temperature and Height Above Background For Alkali and Mixed Alkali Peaks. . . . .	11



## I. INTRODUCTION

### (A) Single Alkali Glasses

Single alkali silicate glasses exhibit two well-known internal friction peaks.<sup>(1-4)</sup> The first peak, hereafter referred to as the alkali peak, is known to correspond in activation energy and frequency with the electrical migration losses due to alkali ions.<sup>(5)</sup> Consequently, it has been attributed to the stress induced movement of the alkali ions.<sup>(6&7)</sup> The alkali peak height also correlates with the sodium diffusion coefficient in sodium aluminosilicate glasses.<sup>(8)</sup> In a theory for the internal friction in ionic conductors, including glasses, Doremus<sup>(9)</sup> recently postulated that the alkali peak should be sensitive to changes in the alkali concentration near the surface. Several mechanisms have been proposed for the second peak occurring at higher temperatures. It has been associated with the stress induced movement of nonbridging oxygen ions<sup>(10,4)</sup>, an interaction between the alkali ions, bridging protons and oxygen ions<sup>(11)</sup> and the diffusion of hydrogen ions.<sup>(12)</sup>

### (B) Mixed Alkali Glasses

When a second alkali oxide is added to a glass, the mixed alkali glass exhibits a new mechanical relaxation<sup>(13-16)</sup> hereafter referred to as the mixed alkali peak. Rötger<sup>(17)</sup>

and Jagdt<sup>(7)</sup> assumed that the mixed alkali peak resulted from an increase in the magnitude of the original peak and its movement to higher temperatures. Steinkamp et al.<sup>(18)</sup>, using small additions of a second alkali, found that the large increase in internal friction was a new peak, unrelated to the alkali peak.

McVay and Day<sup>(19)</sup> reported that the maximum height for the mixed alkali internal friction peak occurs at the composition where the diffusion coefficients for the two alkali ions are equal. It was proposed<sup>(16&19)</sup> that a cooperative rearrangement of dissimilar alkali ions is the mechanism for the mixed alkali damping maximum, with the slower ion controlling the rate of rearrangement. A pair of dissimilar alkali ions is considered to form an elastic dipole, which changes position so as to reduce the magnitude of the applied stress. This mechanism seems to be electrically inactive in mixed alkali silicate glasses.

#### (C) Ion Exchange and Internal Friction

The hypothesis that ion exchange could occur in glass was first suggested after the demonstration of ion exchange in natural silicate minerals such as zeolites. Horovitz<sup>(20&21)</sup> formulated the first ion exchange theory for glass electrodes, which Nikolsky and co-workers<sup>(22-24)</sup> subsequently developed more fully. Ion exchange attracted general attention, resulting in a major practical application, only

after ion exchange techniques were developed for the chemical strengthening of glasses.<sup>(25-28)</sup> Aluminosilicate glasses have been successfully strengthened to 70 Kg/mm<sup>2</sup> and remained resistant to abrasion.<sup>(26&28)</sup>

There are only limited data for the internal friction of ion exchanged glasses. Taylor and Rindone<sup>(29)</sup> and Shelby<sup>(30)</sup> measured the internal friction of ion exchanged alkali silicate glasses. Taylor and Rindone noted the similarity between the internal friction of an annealed ion exchanged and a conventionally melted mixed alkali silicate glass. Shelby indicated that partially ion exchanged alkali silicate glasses exhibit internal friction curves characteristic of a composite of a mixed alkali and single-alkali silicate glass. However, the alkali concentration profiles and degree of ion exchange were not determined in either study.<sup>(29&30)</sup>

De Waal<sup>(31&32)</sup> measured the internal friction of sodium disilicate fibers which had been ion exchanged in a fused salt bath containing lithium or silver ions. He showed that the mixed alkali peak of ion exchanged glasses develops only after the fibers have been reheated briefly to a temperature higher than 200°C. A small but permanent structural modification (formation of intermediate sites was suggested), to adjust to the changed composition, seemed necessary to produce the mixed alkali effect. Reheating the ion exchanged glass to 275°C was believed to

cause a transformation of normal sodium sites to intermediate sites, the features of which are somewhere between those of normal sodium sites and those of normal lithium (or silver) sites.

Both de Waal<sup>(31)</sup> and Taylor and Rindone<sup>(29)</sup> showed that dissolving the ion exchanged layer in acid restored the internal friction of the ion exchanged fiber.

## II. OBJECTIVE OF INVESTIGATION

An investigation of progressively ion exchanged glasses was undertaken in order to gain a better understanding of the internal friction peaks exhibited by these glasses. Since ion exchanged glasses are actually mixed alkali glasses, the internal friction of glasses having the same overall composition, but prepared by ion exchange and conventional melting, could be compared.

Ion exchanged glasses are characterized by a non-uniform alkali ion distribution, and therefore have the advantage of having the mixed alkali region (outer surface) separated from the single alkali region (interior). The effect of the alkali distribution on the internal friction peaks in ion exchanged glasses could be studied since the alkali distribution can be changed by (1) varying the degree of ion exchange, (2) heat treatment after ion exchange, and (3) gradually dissolving the mixed alkali surface layer. Lithium aluminosilicate glasses having an aluminum to total alkali ratio of one, were studied because of their relatively simple structure (absence of non-bridging oxygen), ease of ion exchange, and technical importance.

A recent theory developed by Doremus<sup>(9)</sup> predicts that the alkali internal friction peak should be sensitive to

differences in the alkali concentration at the glass surface. Ion exchange techniques provide a means of testing this theory experimentally.

### III. EXPERIMENTAL PROCEDURE

#### (A) Sample Preparation

A  $\text{Li}_2\text{O}\cdot\text{Al}_2\text{O}_3\cdot 2\text{SiO}_2$  glass (batch composition) was prepared from reagent-grade  $\text{Li}_2\text{CO}_3$ ,  $\text{Al}_2\text{O}_3$ , and potter's flint (99.98% $\text{SiO}_2$ ). The glass was melted in platinum crucibles at  $1550^\circ\text{C}$  in an electric furnace open to the atmosphere. After complete fusion, the melt was stirred several times with a fused silica rod. Fibers approximately 0.4 mm in diameter were then drawn from the melt and stored in glass tubes containing a desiccant.

#### (B) Ion Exchange

Chilled fibers (about 0.4 mm in diameter and 100 mm in length) were ion-exchanged in a reagent grade sodium nitrate bath at  $366 \pm 1^\circ\text{C}$ . The sodium nitrate bath was stirred continuously. After ion exchange the fibers were cooled, rinsed with distilled water to remove the frozen nitrate salt, carefully dried, and stored in a desiccator.

#### (C) Internal Friction Measurements

The internal friction of chilled (unless otherwise specified) ion-exchanged fibers was measured from  $-150^\circ\text{C}$  to  $400^\circ\text{C}$  in an inverted torsion pendulum apparatus<sup>(33)</sup> operating at a frequency of about 0.5 Hz. The procedure followed was identical with that described by Shelby and

Day.<sup>(34)</sup> The temperature gradient over the 70 mm length of the fiber was monitored continuously, by three chromel-alumel thermocouples, and never exceeded 3°C. The heating rate was about 1.5°C/minute.

The internal friction of a rectangular glass specimen (13 x 6 x 114 mm) was measured by Forster's method as described by Moore.<sup>(35)</sup> The temperature gradient along the specimen, as determined by three thermocouples imbedded in a glass bar adjacent to the specimen, never exceeded 5°C.

The internal friction was calculated from the equation:

$$Q^{-1} = \frac{1}{N\pi} \ln (\text{amplitude ratio}) \quad (1)$$

where

$$Q^{-1} = \text{internal friction}$$

$$N = \text{number of cycles}$$

amplitude ratio (or velocity ratio) = ratio of the amplitude of vibrations on the zeroth cycle and the Nth cycle.

The precision of the internal friction was  $\pm 0.1 \times 10^{-3}$  for the torsion pendulum apparatus. The precision in measuring the period of vibration was 0.03%.

(see Appendix A for additional information)

#### (D) Chemical Analysis

After measuring the internal friction of an ion exchanged fiber, the lithium and sodium concentration in the same fiber was determined using a Perkin Elmer 303



Atomic Absorption Spectrophotometer. Successive layers, about 10 $\mu$ m thick, were dissolved in a 5% HF solution. The alkali concentration was determined by comparison with standard solutions. The interference effects caused by the partial ionization of sodium in the air-acetylene flame were avoided by adding a fixed excess amount of potassium (1000  $\mu$ g/ml) to both the standard and sample solutions<sup>(36)</sup>. Robinson<sup>(37)</sup> found no ionization interference on 10 p.p.m. Na by 5,000 p.p.m. K or Li. The thickness of the removed layer was determined from the weight difference before and after etching, the surface area exposed to the acid solution, and an average glass density (2.451 g/cm<sup>3</sup>). Precision of the analysis is  $\pm$  1%.

(see Appendix B for additional information).

## IV. RESULTS

(A) Change in Internal Friction With Progressive Ion-Exchange

Fig. 1 shows the internal friction, as a function of temperature, for chilled  $\text{Li}_2\text{O}\cdot\text{Al}_2\text{O}_3\cdot 2\text{SiO}_2$  glass fibers after various periods of ion exchange in sodium nitrate at  $366^\circ\text{C}$ . The unexchanged fiber exhibits one damping maximum (alkali peak) at  $-25^\circ\text{C}$ . With the replacement of lithium by sodium, a new damping maximum (mixed alkali peak) appears at about  $+90^\circ\text{C}$ . The growth of the mixed alkali peak is accompanied by a reduction in the size of the original alkali peak. After 60 minutes of ion exchange, the alkali peak is only a small shoulder on the low temperature side of the mixed peak. The temperature of the alkali and mixed alkali peaks show little change during ion exchange (Table I).

The sodium content as well as the maximum depth of penetration increases with ion exchange time as shown in Fig. 2.

An interdiffusion coefficient at  $366^\circ\text{C}$  was calculated, from the data of figure 2, according to the following equation<sup>(38 & 39)</sup>

$$C = C_0 \operatorname{erfc} \left( \frac{X}{(4Dt)^{1/2}} \right)$$

where,

C = concentration of sodium at a distance X from the surface

TABLE I

Temperature and Height Above Background For Alkali and Mixed Alkali Peaks

Period of Ion Exchange (minutes)	Alkali Peak			Mixed Alkali Peak			Average Fiber Diameter ( $\pm 5\mu\text{m}$ )	Total $\text{Na}_2\text{O}$ Content** (mole %)
	Height $Q^{-1} \times 10^3$ ( $\pm 0.1$ )	Temperature ( $\pm 2^\circ\text{C}$ )	$f_a^*$ (Hz)	Height $Q^{-1} \times 10^3$ ( $\pm 0.1$ )	Temperature ( $\pm 3^\circ\text{C}$ )	$f_m^*$ (Hz)		
0	13.6	-25	0.49	Not	Observed		350	0
1	12.1	-25	0.51	3.9	+98	0.50	355	0.45
3	10.2	-30	0.51	5.1	+90	0.50	363	- - -
5	8.4	-30	0.49	7.1	+90	0.48	343	1.58
10	8.0	-28	0.57	9.3	+92	0.55	408	- - -
15	6.4	-25	0.49	10.4	+95	0.47	355	2.47
30	4.0	-25	0.51	14.1	+90	0.49	370	3.41
60	1.9	-25	0.42	17.7	+90	0.41	335	5.66
120	1.0	-25	0.50	19.3	+93	0.48	367	6.18
300	Not	Observed		21.5	+95	0.52	370	7.95

\* $f_a$  and  $f_m$  are the frequency at the alkali and mixed peak maximum, respectively.

\*\* After subtracting the  $\text{Na}_2\text{O}$  impurity content (0.69 mole%) of the unexchanged fiber

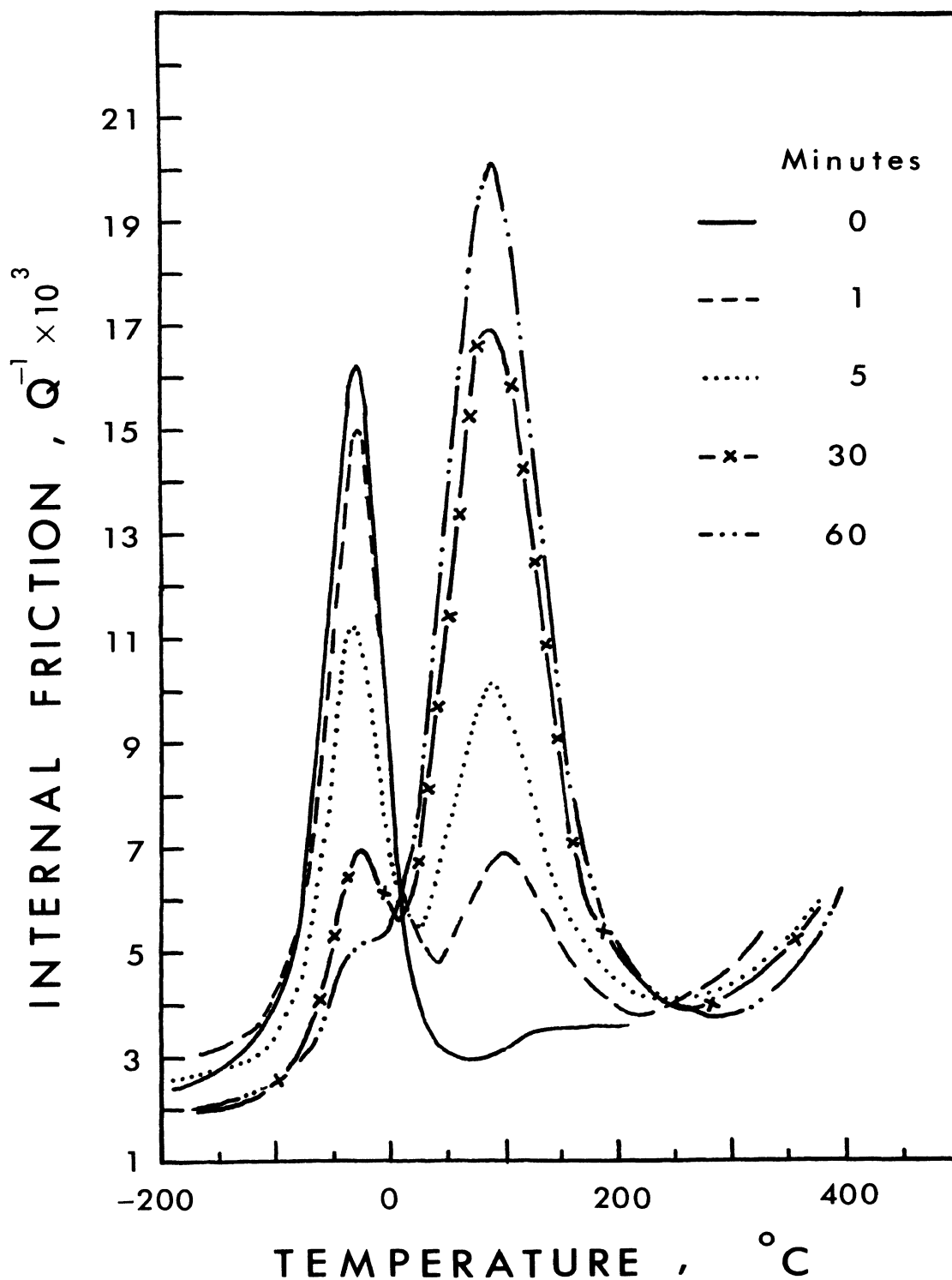


Fig. (1) Internal friction of sodium exchanged chilled  $Li_2O \cdot Al_2O_3 \cdot 2SiO_2$  glass fibers after various periods of time in  $NaNO_3$  bath at  $366^{\circ}C$  ( $f = 0.5$  Hz; diameter =  $350 \pm 15 \mu m$ ).

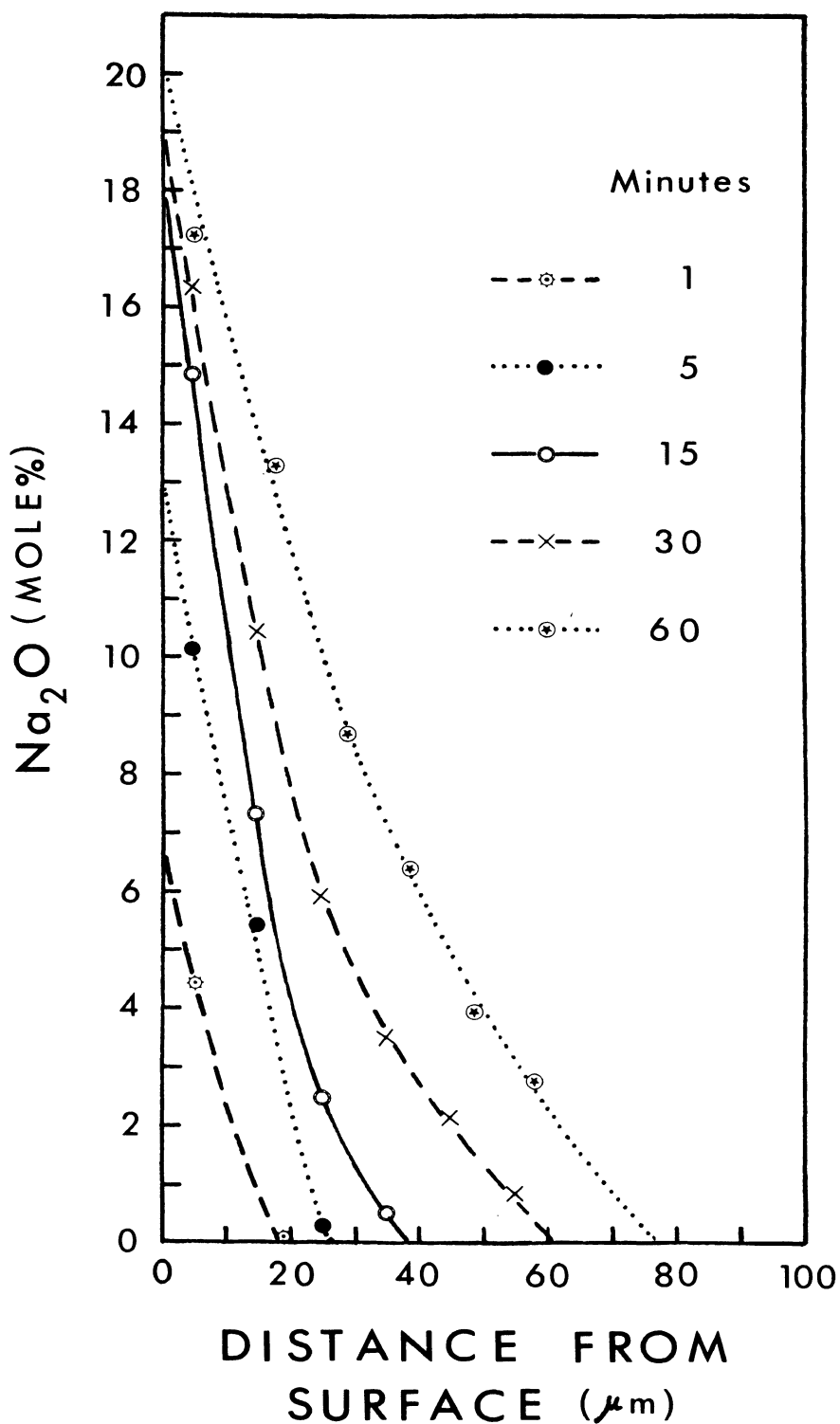


Fig. (2) Concentration of sodium oxide in chilled  $\text{Li}_2\text{O}\cdot\text{Al}_2\text{O}_3\cdot 2\text{SiO}_2$  glass fibers after various periods of time in  $\text{NaNO}_3$  bath at  $366^\circ\text{C}$ .

$C_0$  = concentration of sodium at  $X=0$

erfc = complementary error function

$X$  = distance from surface in cm.

$D$  = diffusion coefficient

$t$  = diffusion time in seconds

The inverse complementary error function of  $C/C_0$  therefore varies linearly with penetration depth ( $X$ ), Fig. 3, and has a slope of  $(4Dt)^{-1/2}$ . The interdiffusion coefficient was almost constant within experimental error:  $2.06 \times 10^{-9}$  (5 minutes),  $1.41 \times 10^{-9}$  (15 minutes),  $1.91 \times 10^{-9}$  (30 minutes) and  $1.73 \times 10^{-9}$   $\text{cm}^2/\text{sec}$ . (60 minutes) the average value being  $1.78 \pm 0.1 \times 10^{-9}$   $\text{cm}^2/\text{sec}$ . at  $366^\circ\text{C}$ .

(B) Change in Internal Friction with Removal of Ion-Exchanged Layer

The effect of dissolving the ion-exchanged surface layer from a chilled fiber (30 minutes in  $\text{NaNO}_3$ ) in 5% reagent grade HF solution is depicted in Fig. 4. After removing a  $23 \mu\text{m}$  layer, the alkali peak became larger while the mixed alkali peak became smaller. Removal of a  $50 \mu\text{m}$  layer resulted in almost restoring the internal friction of the un-exchanged glass. Fig. 5 shows the corresponding sodium oxide concentration profiles.

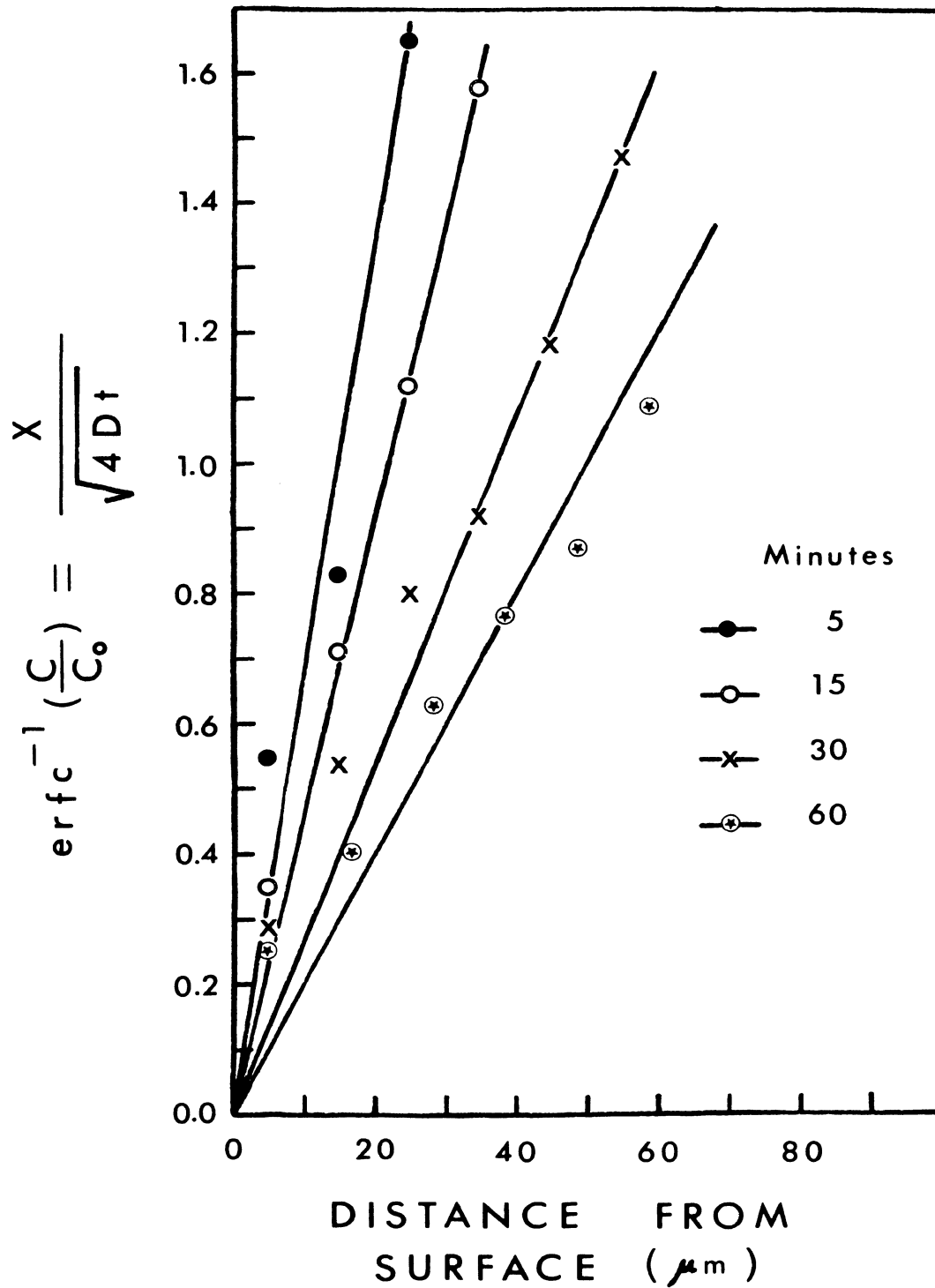


Fig. (3) Inverse complementary error function of Na relative concentration vs. distance from the surface.

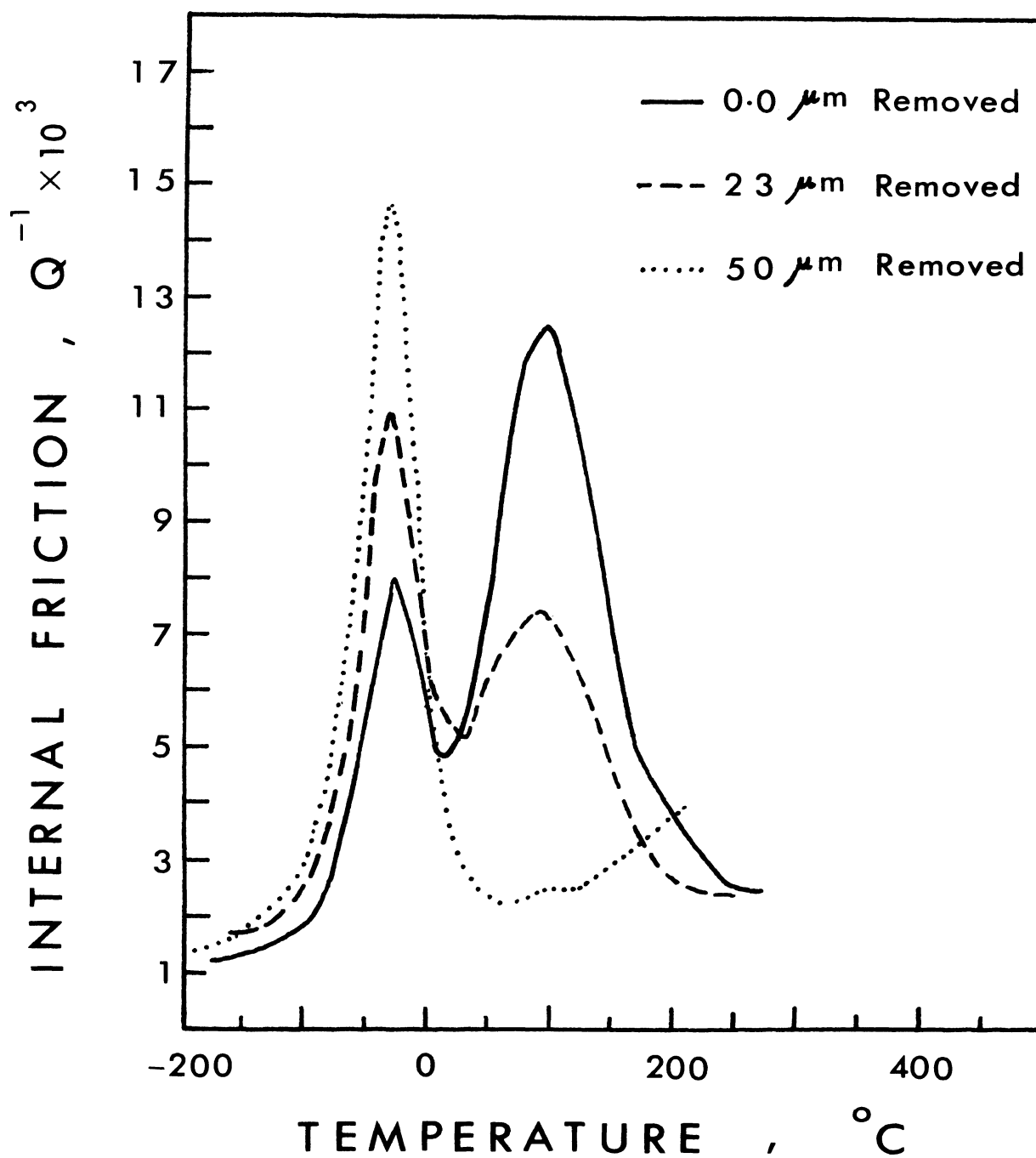


Fig. (4) Internal friction of a sodium exchanged  $\text{Li}_2\text{O} \cdot \text{Al}_2\text{O}_3 \cdot 2\text{SiO}_2$  glass fiber (30 minutes in  $\text{NaNO}_3$  at  $366^{\circ}\text{C}$ ) before and after removing various amounts of ion-exchanged layer ( $f = 0.41 - 0.74$  Hz; original fiber diameter =  $450\mu\text{m}$ ).



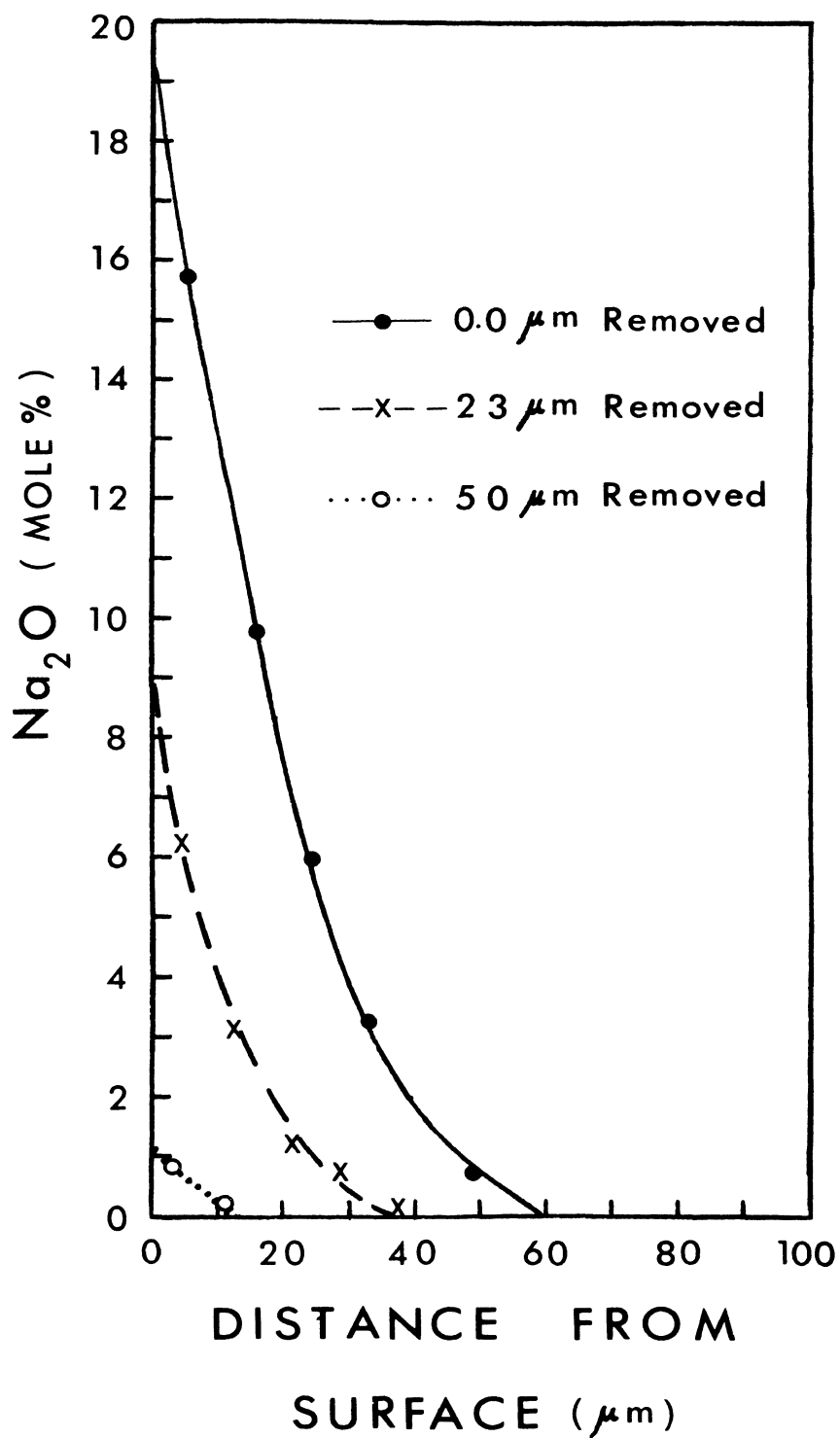


Fig. (5) Concentration of sodium oxide after removing various amounts of ion-exchanged layer.

(C) Effect of Sample Dimension on Internal Friction

In the preliminary ion exchange experiments, the magnitude of the alkali and mixed alkali peaks did not vary systematically with the degree of ion exchange. In order to determine whether the internal friction was dependent upon the diameter of the fiber, three fibers of different diameter were simultaneously ion exchanged in sodium nitrate for 30 minutes. The chilled fibers received no heat treatment after ion exchange. Fig. 6 shows that with decreasing fiber diameter, the alkali peak became smaller while the mixed alkali peak became larger. The  $\text{Na}_2\text{O}$  and  $\text{Li}_2\text{O}$  concentration profiles shown in Fig. 7 for these three fibers are identical within experimental error. Chemical analysis showed that the total alkali content ( $\text{Na}_2\text{O} + \text{Li}_2\text{O}$ ) remained constant at about 25 mole percent with increasing distance from the fiber surface.

A further example of the dependence of the internal friction on sample size was obtained from the comparison of a rectangular glass bar (13 x 6 x 114 mm) and a fiber (0.37 mm in diameter) simultaneously ion-exchanged for 30 minutes at  $366^\circ\text{C}$ . The internal friction for the glass bar, shown in Fig. 8, is characterized by an alkali peak at  $+75^\circ\text{C}$  (magnitude =  $8.5 \times 10^{-3}$ ). The very small inflection at  $+255^\circ\text{C}$  corresponds to the mixed alkali peak. The fiber, however, exhibits a small alkali peak at  $-25^\circ\text{C}$  and a large mixed alkali peak at  $+90^\circ\text{C}$ . Neither sample was heat

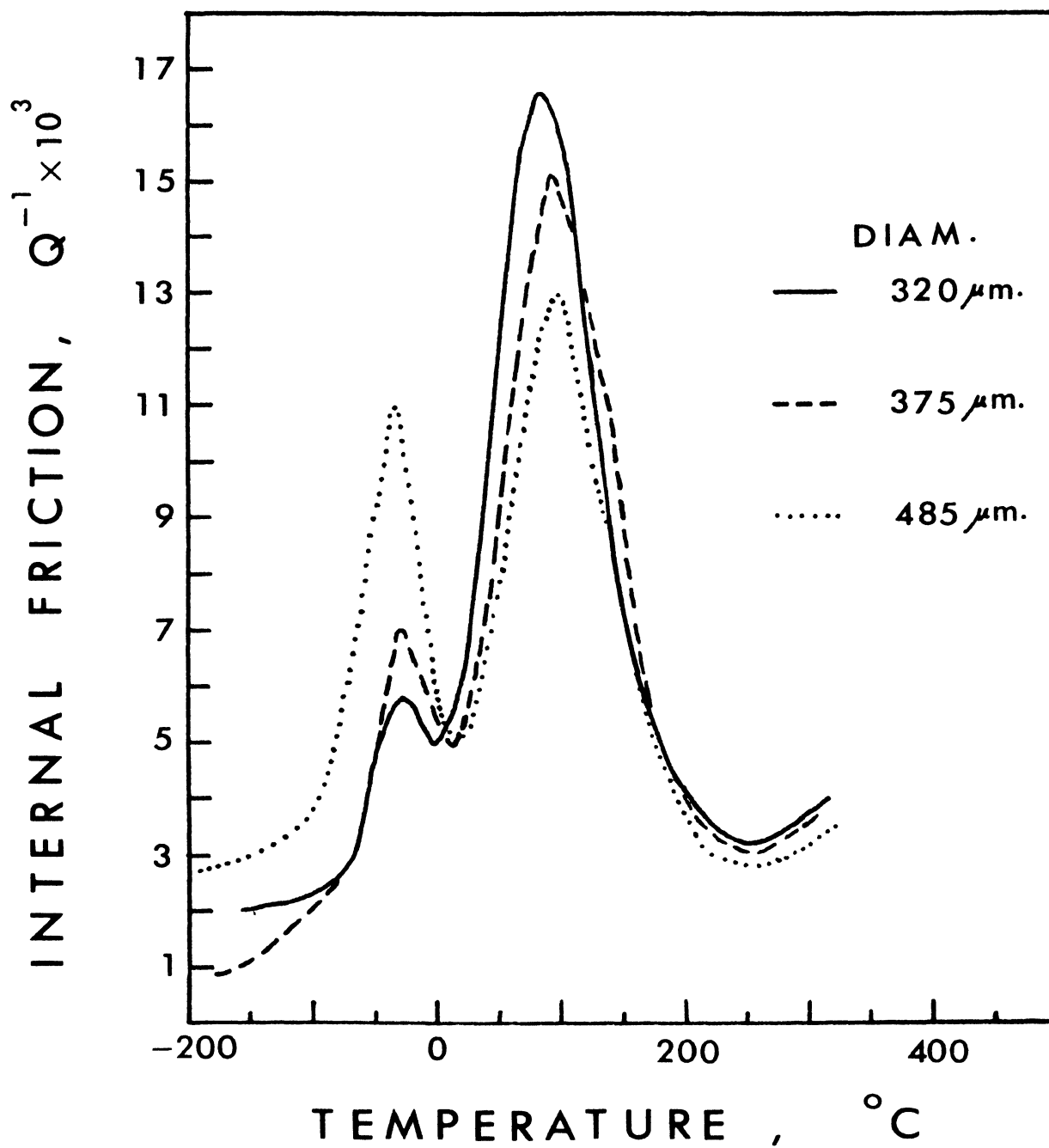


Fig. (6) Internal friction for sodium exchanged  $Li_2O \cdot Al_2O_3 \cdot 2SiO_2$  glass fibers, 30 minutes in  $NaNO_3$  Bath at  $366^{\circ}C$  ( $f = 0.37, 0.59, 0.78$  Hz).

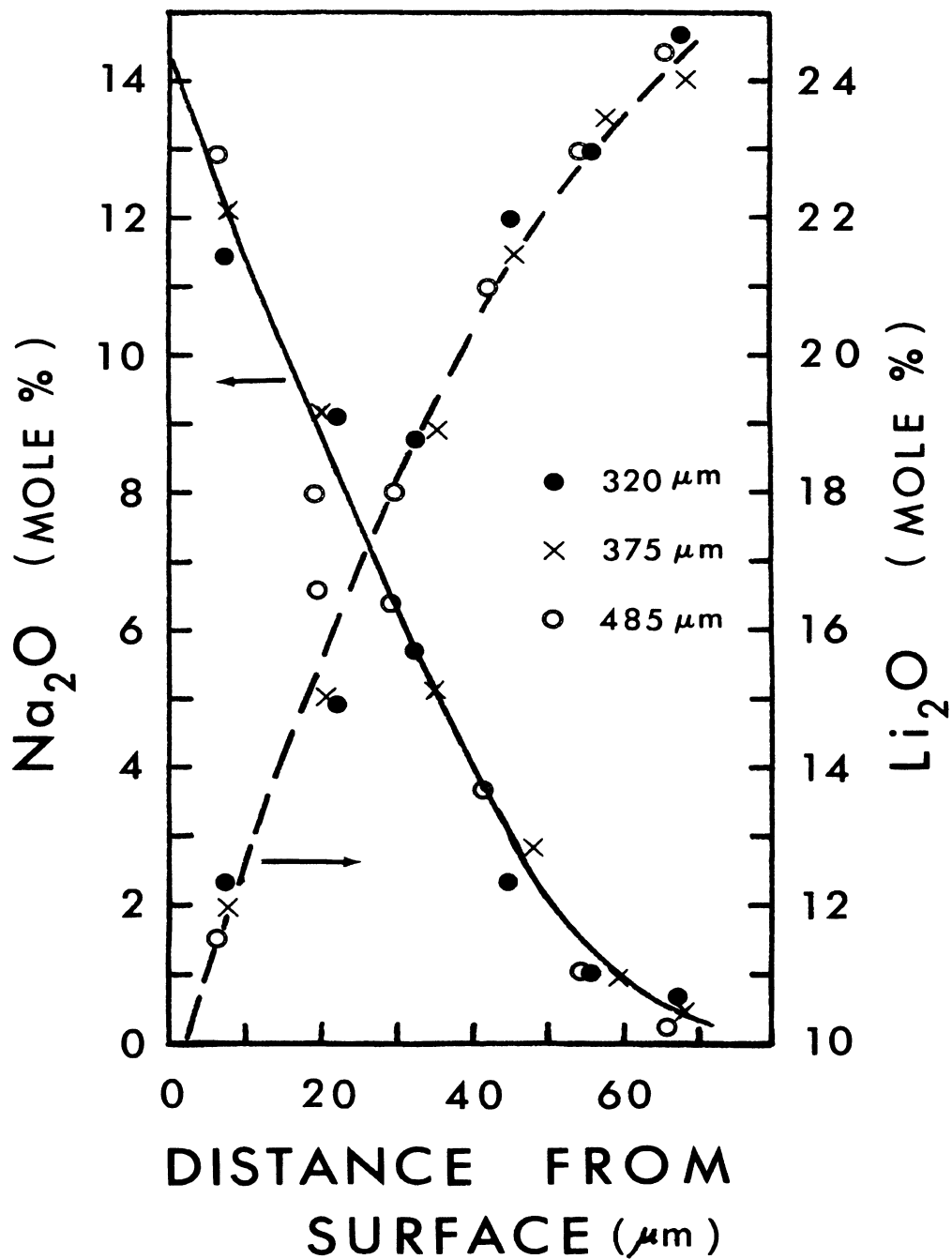


Fig. (7) Concentration of sodium oxide (solid line) and lithium oxide (dashed line) in sodium exchanged  $\text{Li}_2\text{O}\cdot\text{Al}_2\text{O}_3\cdot 2\text{SiO}_2$  glass fibers after 30 minutes in  $\text{NaNO}_3$  bath at  $366^\circ\text{C}$ . Fiber diameters =  $320\mu\text{m}$ (●),  $375\mu\text{m}$ (x), and  $485\mu\text{m}$ (o).

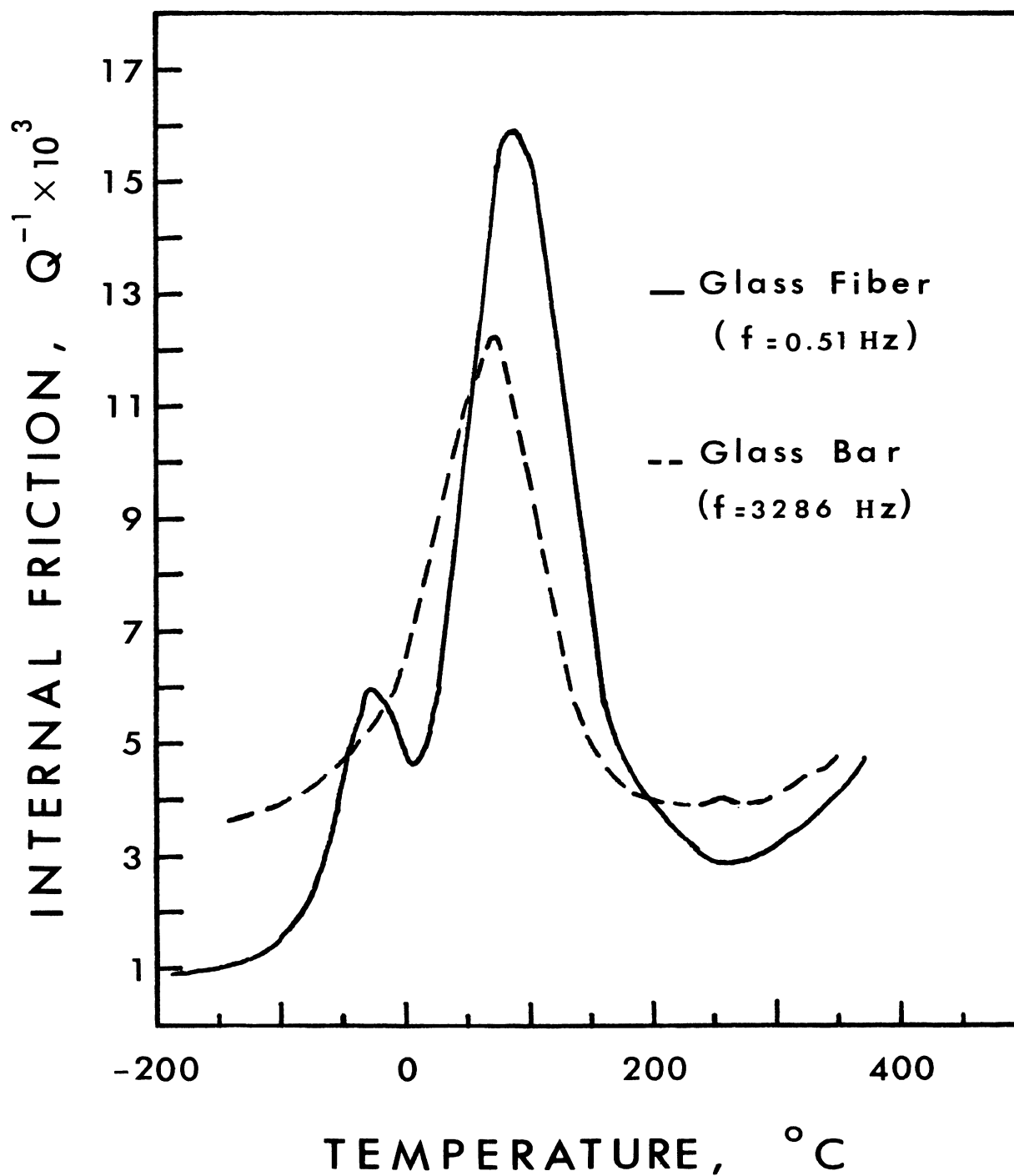


Fig. (8) Internal friction for sodium exchanged  $Li_2O \cdot Al_2O_3 \cdot 2SiO_2$  glass fiber (diameter =  $370\mu m$ ) and glass bar ( $13 \times 6 \times 114$  mm) after 30 minutes in  $NaNO_3$  bath at  $366^{\circ}C$ .

treated after ion exchange.

(D) Internal Friction of Glasses Prepared by Different Techniques

Heating an ion-exchanged glass at an elevated temperature produces a uniform distribution of the alkali ions similar to that in a conventionally melted mixed alkali glass. The total lithium and sodium content of the ion-exchanged glass was determined by chemical analysis and a glass was melted with the same composition ( $0.9 \text{ Li}_2\text{O} \cdot 0.1 \text{ Na}_2\text{O} \cdot \text{Al}_2\text{O}_3 \cdot 2\text{SiO}_2$ ). In order to compare the internal friction of fibers from glasses prepared by these two techniques, the conventionally melted glass was stabilized at  $590^\circ\text{C}$  for 3 hours and the glass to be ion-exchanged was stabilized at the same temperature before ion exchange in  $\text{NaNO}_3$  for 15 minutes at  $366^\circ\text{C}$ . After ion-exchange it was heat treated again at  $590^\circ\text{C}$  for 3 hrs. Its internal friction is shown by the solid curve in Fig. 9. The internal friction of the conventionally melted glass is represented by the dashed curve. Both fibers, having the same composition but prepared by two different techniques, show essentially the same internal friction.

(E) Effect of Alkali Ion Distribution on Internal Friction

The dependence of the internal friction upon the sodium ion distribution was determined from fibers whose sodium ion distribution had been varied by heat treatment at  $590^\circ\text{C}$ .

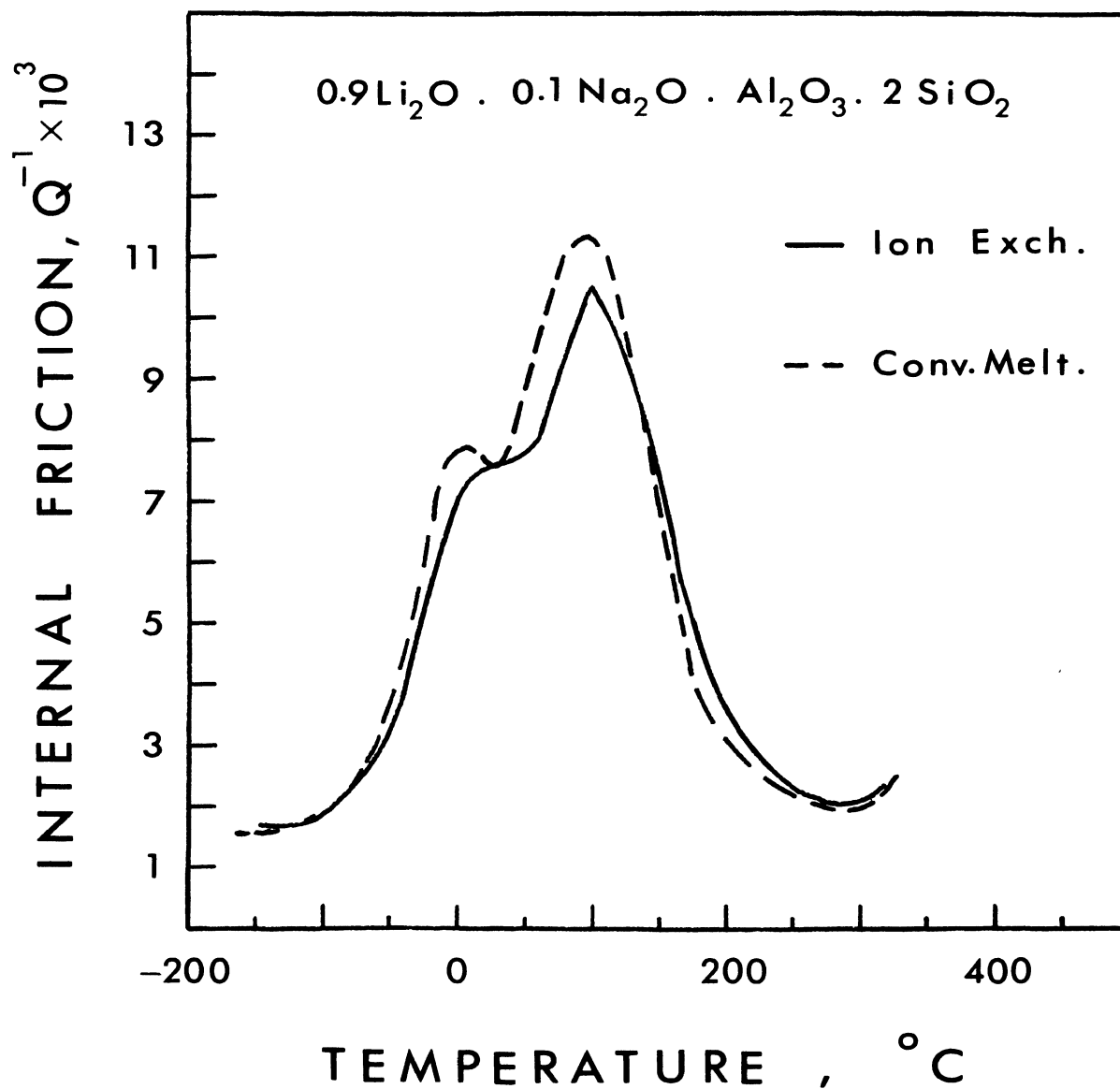


Fig. (9) Internal friction for a sodium exchanged (15 minutes in  $\text{NaNO}_3$  at  $366^\circ\text{C}$ ) and a conventionally melted fiber of same composition ( $f \approx 0.6$  Hz).

The network structure of three  $\text{Li}_2\text{O}\cdot\text{Al}_2\text{O}_3\cdot 2\text{SiO}_2$  glass fibers was stabilized by heat treatment at  $590^\circ\text{C}$ . The fibers were then ion exchanged for 15 minutes in  $\text{NaNO}_3$  at  $366^\circ\text{C}$ , the sodium ions penetrating to a depth of about  $40\mu\text{m}$  (solid curve in Fig. 10). One fiber was further heat treated at  $590^\circ\text{C}$  for 10 minutes, thereby reducing the sodium concentration gradient (dashed curve). Three hours at  $590^\circ\text{C}$  resulted in a uniform distribution of the lithium and sodium ions, i.e. in a homogeneous fiber (dotted curve).

The changes in the internal friction corresponding to the different sodium concentration profiles are shown in Fig. 11. The magnitude and position of the mixed alkali peak was unaffected by changing the alkali distribution. However, the alkali peak was reduced and shifted to higher temperatures by the heat treatment at  $590^\circ\text{C}$ .

Fig. 12 shows the mixed alkali peak for a chilled fiber ( $370\ \mu\text{m}$  diameter) after being ion-exchanged in sodium nitrate for 5 hours. After 3 hours heat treatment at  $590^\circ\text{C}$ , the mixed alkali peak shifted to lower temperatures (from  $+95$  to  $+75^\circ\text{C}$ ) and became slightly larger (from  $21.5$  to  $22.5 \times 10^{-3}$ ).

(see Appendix C for other related results).



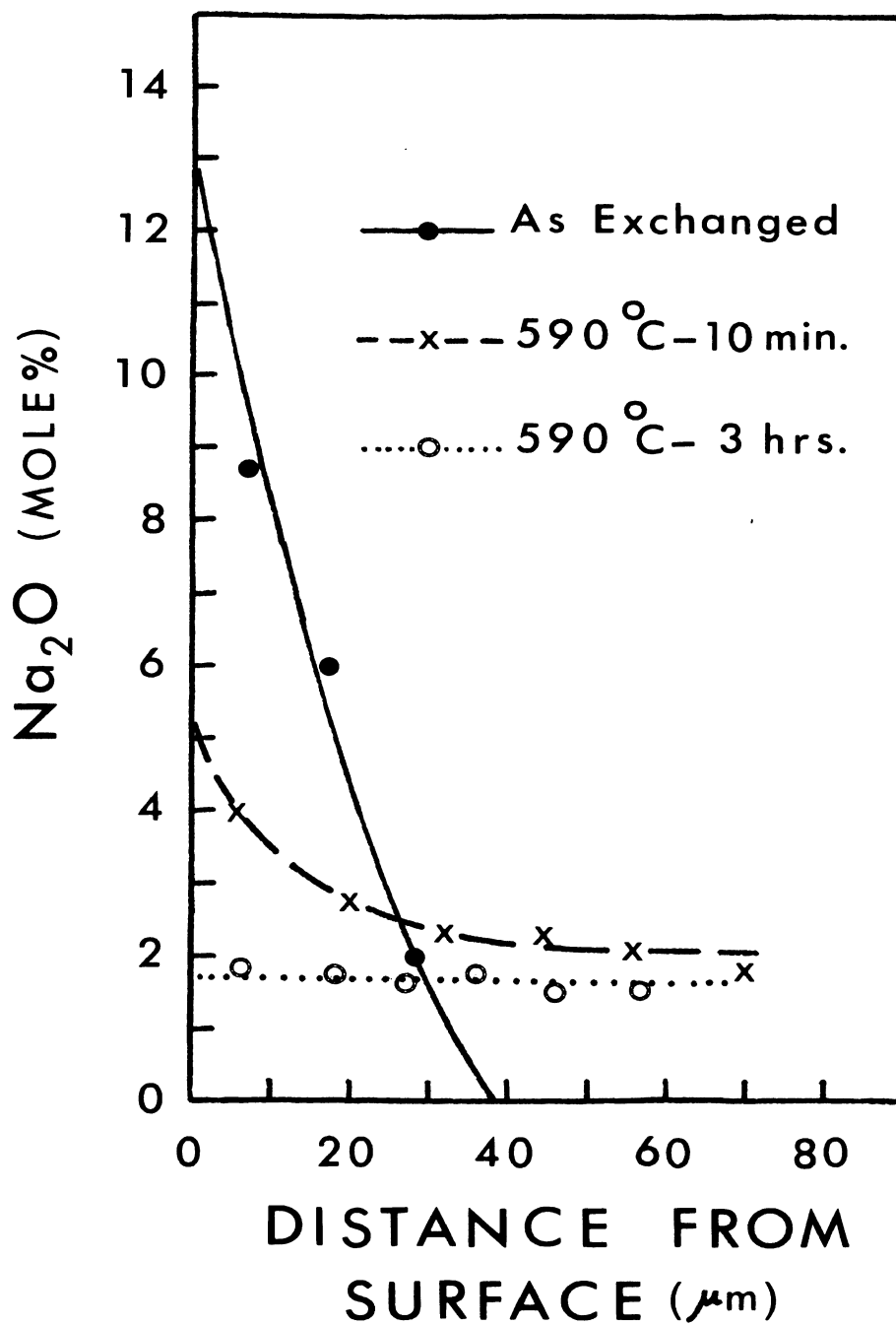


Fig. (10) Sodium oxide concentration profiles in a sodium exchanged  $\text{Li}_2\text{O}\cdot\text{Al}_2\text{O}_3\cdot 2\text{SiO}_2$  glass fiber (15 minutes in  $\text{NaNO}_3$  at  $366^\circ\text{C}$ ) heat treated at  $590^\circ\text{C}$  before and after ion exchange.

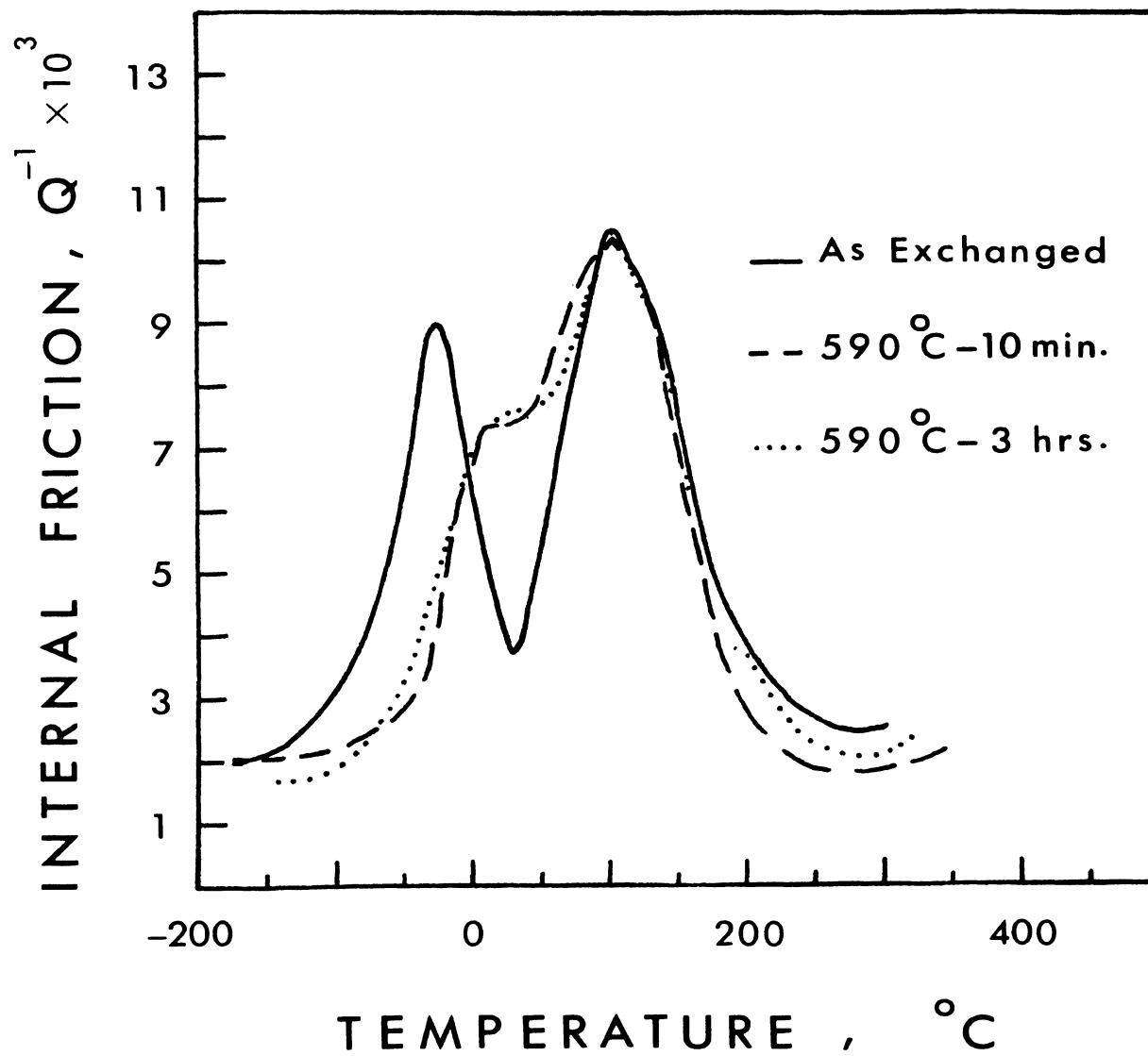


Fig. (11) Internal friction of sodium exchanged  $Li_2O \cdot Al_2O_3 \cdot 2SiO_2$  glass fiber (15 minutes in  $NaNO_3$  at  $366^{\circ}C$ ) heat treated at  $590^{\circ}C$  before and after ion exchange. ( $f = 0.6$  Hz).

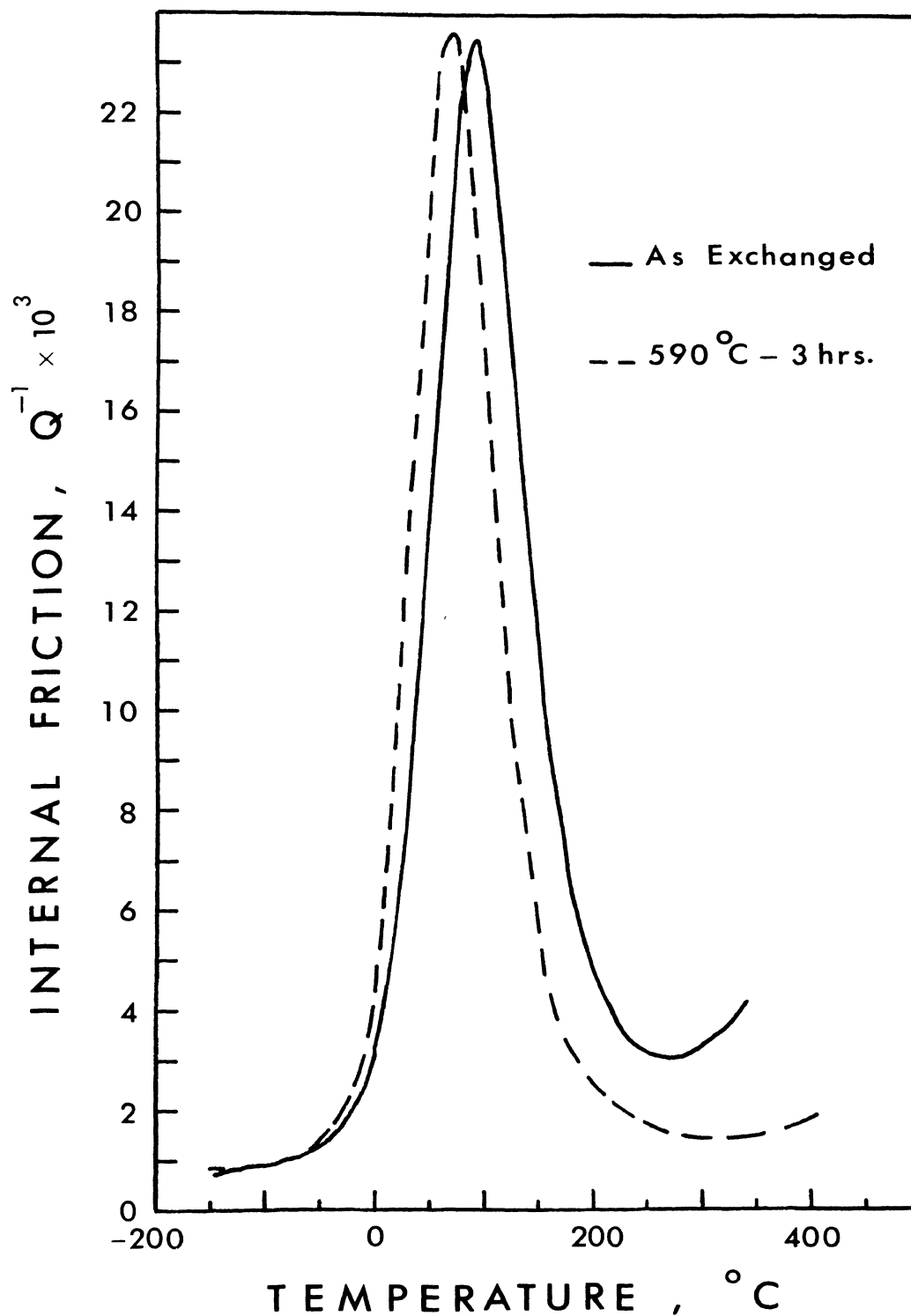


Fig. (12) Internal friction of sodium exchanged chilled  $Li_2O \cdot Al_2O_3 \cdot 2SiO_2$  glass fiber (5 hrs. in  $NaNO_3$  at  $366^{\circ}C$ ) before and after heat treatment at  $590^{\circ}C$  for three hours ( $f = 0.5$  Hz).

## V. DISCUSSION

(A) Change in Internal Friction with Progressive Ion Exchange

Upon the introduction of a second alkali ion - by ion exchange - in de Waal's<sup>(31)</sup> glasses, the internal friction of these glasses was similar to that for comparable glasses prepared by a conventional melting procedure. Hence, the new damping peak (at about 90°C), Fig. 1, which in the ion exchanged glass increases in magnitude with increasing sodium content (Fig. 2) is considered identical with the known mixed alkali peak. The accompanied reduction in the magnitude of the alkali peak is the same we observe in a single alkali glass upon partial replacement of the alkali by another type of alkali ion.

Fig. 13 shows the alkali and mixed alkali peak height as a function of total sodium oxide concentration for chilled ion-exchanged  $(1-x) \text{Li}_2\text{O} \cdot x \text{Na}_2\text{O} \cdot \text{Al}_2\text{O}_3 \cdot 2\text{SiO}_2$  glasses (filled circles) and for annealed  $(1-x) \text{Li}_2\text{O} \cdot x \text{Na}_2\text{O} \cdot \text{Al}_2\text{O}_3 \cdot 6\text{SiO}_2$  glasses prepared by conventional melting (open circles). The data for ion-exchanged glasses are extracted from Fig. 1 and the corresponding chemical analysis. For both the ion exchanged and conventionally melted glasses the alkali peak became smaller while the mixed alkali peak becomes progressively larger, as the total sodium oxide increases. There is, however, a slight difference in the

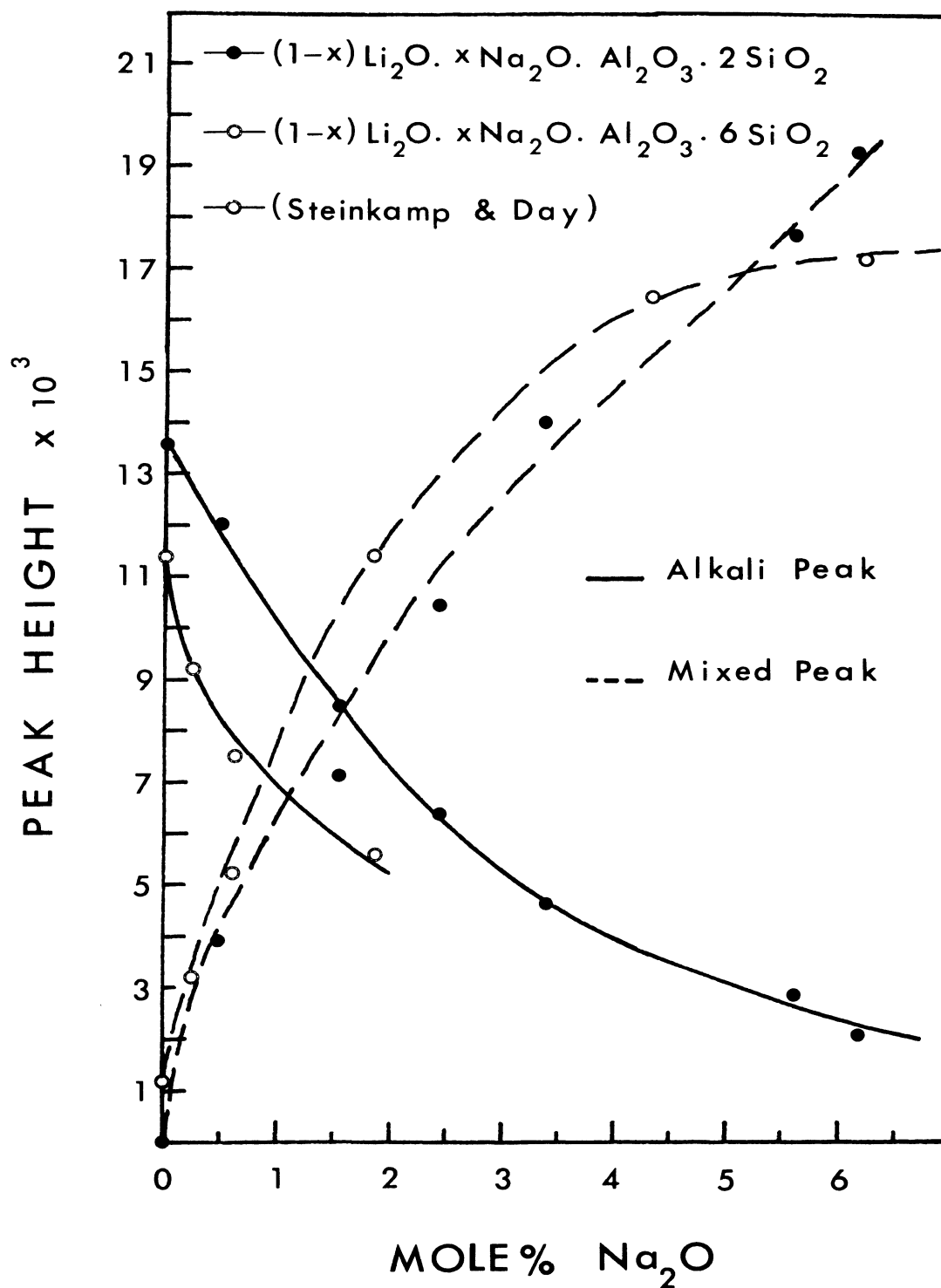


Fig. (13) Comparison of height for alkali peak and mixed alkali peak in ion exchanged (●) and conventionally melted (○) glasses.

peak height because of the compositional difference in the two sets of glasses, namely 12.5 and 25 mole% total alkali. From this comparison, it seems that it is not important to prepare each glass from the melt with each specific cation having its own kind of site and surrounding. The mixed alkali effect, as manifested by changes in the mechanical damping, could be achieved by replacing some of the lithium ions by sodium ions on the same sites by ion exchange.

De Waal<sup>(31)</sup> indicated that in order to observe the mixed alkali peak it is necessary to reheat a glass fiber after ion exchange to a certain temperature, so as to generate what he calls "intermediate sites." In the present study, reheating was found unnecessary.

(B) Change in Internal Friction with Removal of the Ion-Exchanged Layer

The reduction in the mixed alkali peak and the simultaneous increase in the alkali peak upon the gradual removal of the mixed alkali surface layer, (Figures 4 & 5), indicates that the alkali peak is due to the unaffected core. The mixed alkali layer is responsible for the mixed peak. The small shoulder (mixed alkali peak at about 100°C) in the internal friction of the fiber after dissolving 50  $\mu\text{m}$  layer (dotted curve in Fig. 4) corresponds with the small  $\text{Na}_2\text{O}$  concentration near its surface (Fig. 5).

When the mixed alkali peak height of the ion-exchanged fiber (30 minutes at 366°C) is plotted versus the depth of

the removed surface layer (see Fig. 14); it is found to change in a linear fashion. A similar linear decrease of the mixed peak height with the depth of the layer removed from the surface was observed by Taylor<sup>(40)</sup>.

(C) Activation Energy for Internal Friction and Inter-diffusion Coefficient

Previously<sup>(10,4,34)</sup>, the movement of an internal friction peak to lower or higher temperatures was interpreted as indicating a decrease or increase in the activation energy, respectively. This interpretation should be valid as long as the compositional changes responsible for a change in peak temperature do not lead to a different relaxation mechanism. Since the temperatures for the alkali and mixed alkali peak do not change significantly with progressive ion exchange (Fig. 1), the corresponding activation energies are apparently constant. The activation energy for relaxation seems to depend primarily on the network structure. Since the temperature of ion exchange (366°C) is well below the annealing range, there should have been no significant change in the network structure.

For different degrees of ion exchange, from 5 to 60 minutes, the interdiffusion coefficient ( $1.78 \times 10^{-9}$  cm<sup>2</sup>/sec.) remained constant (Fig. 3). This also indicates that the diffusion is primarily controlled by the fixed (rigid) network structure. In other words, the energy barriers for diffusion are not changed significantly with the

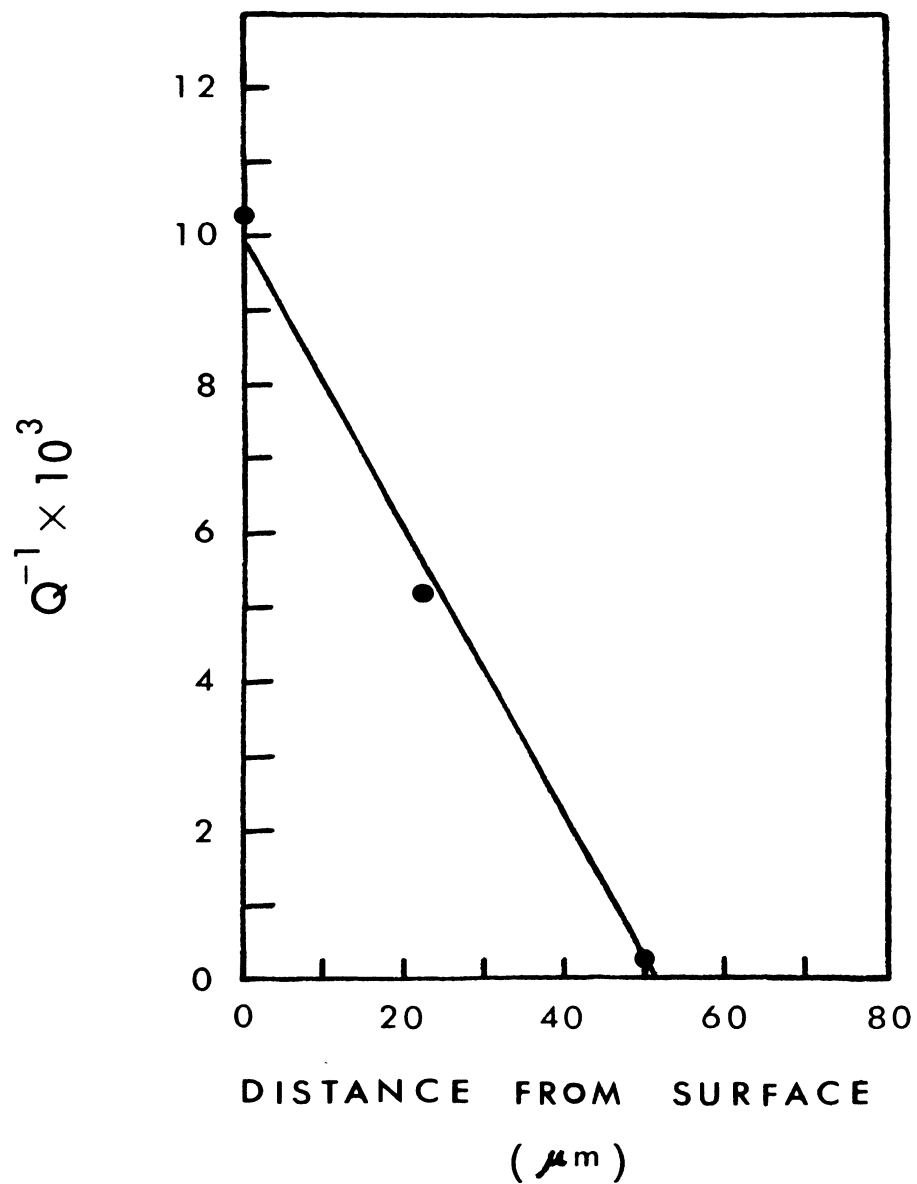


Fig. (14) Mixed alkali peak height vs. thickness of dissolved surface layer for  $\text{Li}_2\text{O} \cdot \text{Al}_2\text{O}_3 \cdot 2\text{SiO}_2$  glass ion-exchanged 1/2 hr. at  $366^\circ\text{C}$  in  $\text{NaNO}_3$  (original diameter =  $450\mu\text{m}$ ).



introduction of sodium.

(D) Relation Between Alkali Peak Height and Sodium Penetration Depth

De Waal<sup>(31)</sup> calculated the reduction in the height of the alkali peak that may be expected theoretically in Ag ion-exchanged sodium disilicate glasses as a function of the penetration depth of the silver ions. He assumes that the ion-exchanged surface layer does not contribute to the alkali peak and the shear modulus is constant along the fiber radius, and develops the equation. (See Appendix D for the derivation of the equation).

$$(\tan \delta / \tan \phi) = (1 - \frac{\rho}{R})^4 = (\frac{r}{R})^4 \quad (2)$$

where,

$\tan \delta$  = internal friction (alkali peak) of ion exchanged glass fiber

$\tan \phi$  = internal friction of the unexchanged fiber

$\rho$  = penetration depth of the second alkali

$r$  = radius of the unaffected core of the fiber

$R$  = overall radius of the fiber

According to Equation (2) silver ions penetrating to a depth of 40  $\mu\text{m}$  would cause a 70% reduction in the original alkali peak height. However, the experimental reduction measured in a fiber not reheated to 275°C amounted to only 5 or 10%. De Waal concluded that the sodium ions in

the surface layer must still be contributing to the alkali peak. After reheating, the reduction in the alkali peak height was in good agreement with Equation (2) and a mixed alkali peak appeared.

The applicability of de Waal's equation to the glasses in Figs. 1 & 2 was examined. Fig. 15 shows the relatively good agreement found between Equation (2) and the experimental data. The experimental alkali peak height is slightly higher than what Equation (2) predicts from the experimentally determined sodium depth of penetration, but this difference could be accounted for if the lithium ions near the ion exchanged interface partially contribute to the alkali peak. This is considered a reasonable assumption, since the lithium concentration is high, while the sodium concentration is low, near the interface. The lithium ions at the interface are still sufficiently mobile to contribute to the alkali peak mechanism.

In the present study it was not necessary to reheat the samples after ion exchange in order for the results to be in good agreement with the Equation (2).

Based on the validity of de Waal's equation, the decrease in magnitude for the alkali peak (Fig. 1) is clearly related to the increase in the depth of penetration of sodium ions (Fig. 2) for fibers with approximately the same radius. On the other hand, in Figures 4 and 5, the alkali peak height increases as the thickness of the ion

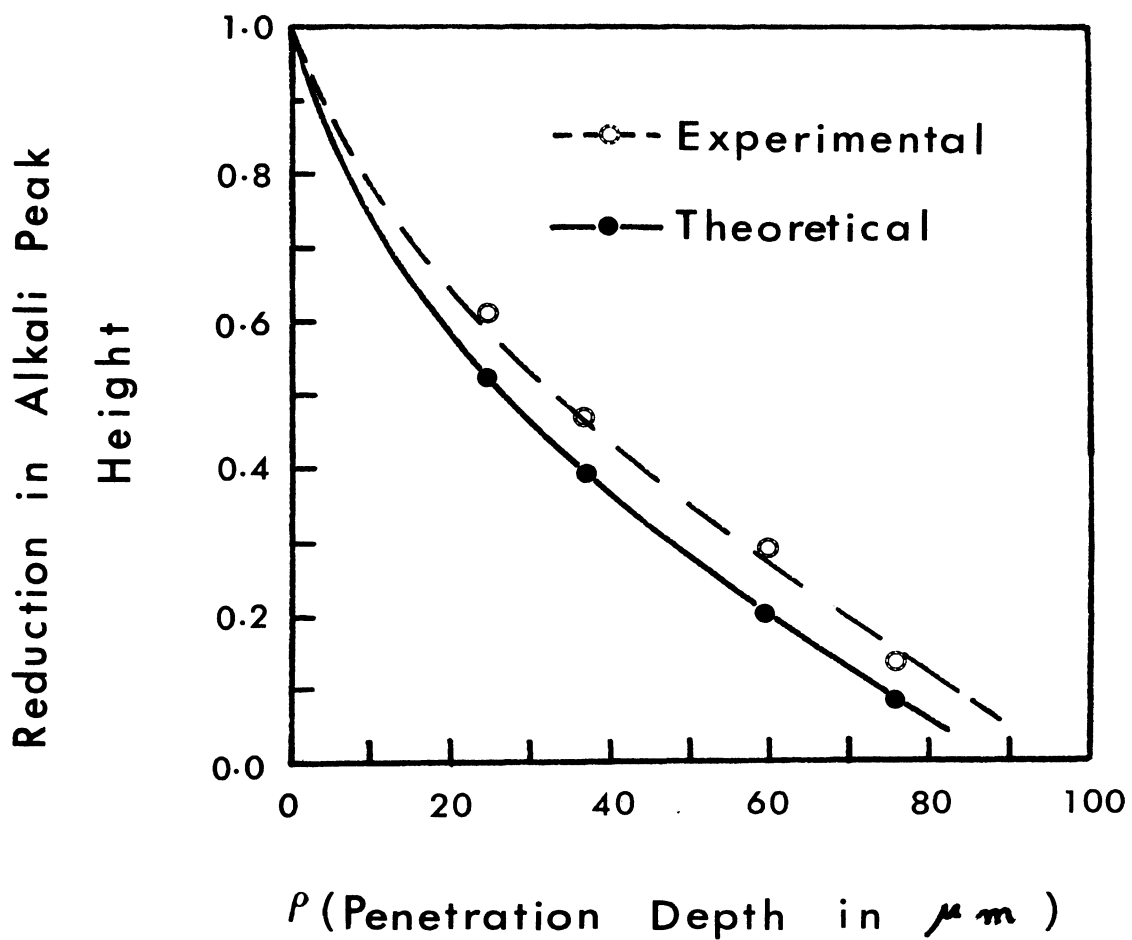


Fig. (15) Reduction in alkali peak height with sodium penetration depth.

exchanged layer ( $\rho$ ) decreases (being gradually dissolved in an HF solution) and the fiber radius ( $R$ ) decreases. When the radius of the unaffected core ( $r$ ) equal the fiber radius ( $R$ ), the magnitude of the alkali peak should be the same as that in the unexchanged glass. Indeed, after dissolving a 50  $\mu\text{m}$  layer, ( $R$ ) almost equals ( $r$ ) and the alkali peak magnitude is almost fully restored (Fig. 4).

The depth of the penetration of a second alkali ion (introduced by ion-exchange) in circular cross sectioned specimen can be obtained fairly accurately by measuring the decrease in magnitude of the alkali peak. This is a non-destructive measurement and represents a practical application of internal friction measurements, that could have value in the chemical strengthening of glasses by ion-exchange methods.

#### (E) Effect of Sample Dimensions on Internal Friction

In conventionally melted glasses the alkali ions are generally uniformly distributed unless the glasses are phase separated. The concentration of the relaxing units per unit volume is constant throughout the sample and the internal friction is independent of the sample dimensions. Ion exchanged glasses, however, have a nonuniform alkali ion distribution. Thus, the concentration of alkali ions per unit volume varies in accordance with the position of these volume elements in the sample.

The three ion-exchanged fibers in Fig. 6 have mixed alkali surface layers, (about  $70\mu\text{m}$  thick) which are exactly alike as far as the sodium and lithium ion concentration gradient is concerned (Fig. 7). The principal difference is the size of the un-exchanged core in each fiber. This core contains only lithium ions and is largest ( $= 345\mu\text{m}$ ) for the  $485\mu\text{m}$  diameter fiber. The  $320\mu\text{m}$  diameter fiber has the smallest un-exchanged core ( $= 180\mu\text{m}$ ). It is easily shown that the larger fiber has more volume elements containing only lithium per total fiber volume than the smaller fiber. According to Equation (2), the larger fiber should have the largest alkali peak since the ratio of the radius of the unaffected core ( $r$ ) to the fiber radius ( $R$ ) is greater for this fiber.

The same argument is applicable, but on a larger scale, to the bar and fiber shown in Fig. 8. Considering the relatively large dimensions of the bar compared to the depth of ion exchange, the bar is essentially un-exchanged. Thus, the presence of only an alkali peak, and practically no mixed alkali peak, is consistent with the extremely low volume fraction of the mixed alkali surface layer. Similarly the large mixed alkali peak and the small alkali peak in the fiber agrees with the volume fractions of the mixed alkali and un-exchanged regions in this specimen. The dependence of the internal friction of ion exchanged glasses upon specimen size, therefore, is related to the relative

volume fractions of the mixed alkali and single alkali regions in the specimen. When the volume fraction of the exchanged regions is low, only the alkali peak may be observed. As the volume fraction of the mixed alkali (exchanged) region increases, then the mixed alkali peak is also detected. Finally, it is concluded that the internal friction peaks of the ion-exchanged glasses are related to the overall composition.

(F) Internal Friction of Glasses Prepared by Different Techniques

The internal friction of conventionally melted and heat treated ion-exchanged glasses of the composition  $0.9 \text{ Li}_2\text{O} \cdot 0.1 \text{ Na}_2\text{O} \cdot \text{Al}_2\text{O}_3 \cdot 2\text{SiO}_2$  was found basically similar (Fig. 9). Similarly, the internal friction of a heated ion-exchanged sodium silicate glass and a conventionally melted glass of nearly the same composition, both determined by de Waal<sup>(31)</sup>, are compared in Fig. 16. The similarity is apparent. The ion-exchanged glass was prepared by ion-exchanging a  $\text{Na}_2\text{O} \cdot 2\text{SiO}_2$  glass for 30 minutes in (Li, Na, K)  $\text{NO}_3$  at  $175^\circ\text{C}$  followed by annealing at  $410^\circ\text{C}$ . The glass prepared by melting was annealed at  $430^\circ\text{C}$  and had lower lithium content, 1.9 mole% as compared to the 2.4 mole% for the ion-exchanged glass. The slight difference in the internal friction peaks is attributed to the small compositional difference between these glasses. The

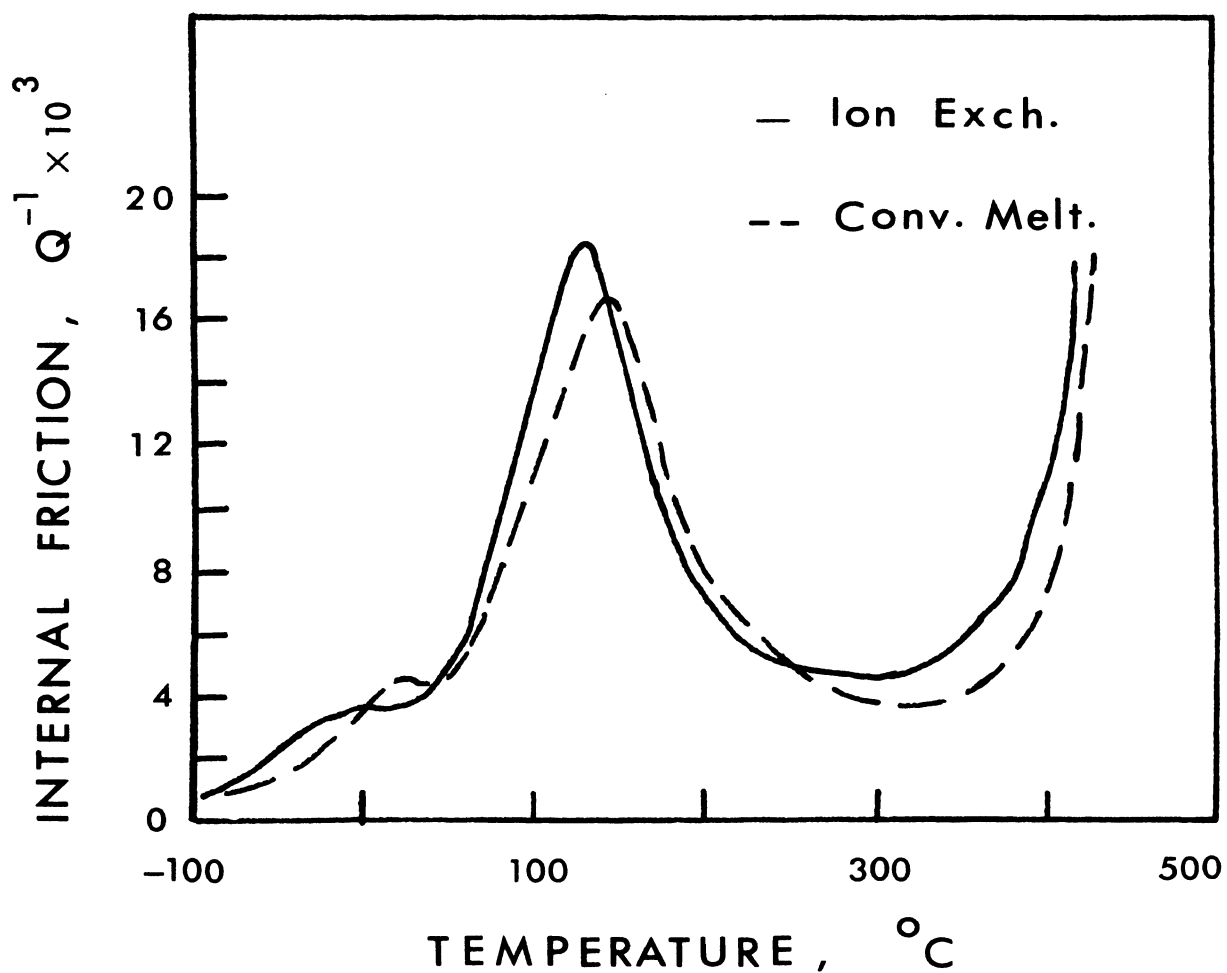


Fig. (16) Internal friction for ion exchanged and conventionally melted glasses. Solid line (30.6%  $Na_2O \cdot 2.4\% Li_2O \cdot 67.0\% SiO_2$ ). Dashed line (30.9  $Na_2O \cdot 1.9\% Li_2O \cdot 67.2\% SiO_2$ ). (After H. de Waal<sup>(31)</sup>).

relaxation spectrum of ion-exchanged glasses has also been related to the overall chemical composition (see Fig. 13).

These results support the conclusion that the mechanical damping of ion-exchanged glasses is dependent on overall composition and is similar to that for conventionally melted glasses of the same composition. This conclusion is further supported by the results of Frischat<sup>(41)</sup>. He reported that ion-exchanged and conventionally melted Na-K aluminosilicate glasses of the same overall composition have essentially the same electrical conductivity. The present internal friction measurements and Frischat's electrical conductivity measurements both indicate that it makes no difference whether the second alkali is uniformly distributed throughout the glass or is confined to a layer on the surface.

(G) Effect of Alkali Ion Distribution on the Internal Friction

The magnitude of the mixed alkali peak did not change (Fig. 11) with the change in concentration profile (Fig. 10) after heat treating the ion-exchanged glass at 590°C for 10 and 180 minutes. The change in concentration profile and the internal friction data shown in Figures 10 and 11 are for fibers which had been stabilized prior to ion-exchange in order to minimize the network relaxation when the glasses were heat treated at 590°C for 3 hours after ion-exchange. From this it appears that the magnitude of



the mixed alkali peak is independent of the change in alkali distribution. This is attributed to the fact that in this case the total number of dissimilar alkali pairs did not change during the heat treatment. This would occur, ideally, if the initial concentration of sodium oxide is nowhere higher than half of the total alkali oxide content (12.5 mole%) as was the case in this experiment (see Fig. 10).

A higher concentration (about 24 mole%) of  $\text{Na}_2\text{O}$  at the surface of the fiber was obtained after 5 hours of ion-exchange in  $\text{NaNO}_3$ . One would expect an increase in the number of dissimilar alkali pairs after the heat treatment at  $590^\circ\text{C}$  for 3 hours due to the further penetration of the sodium ions and the additional pairing in the glass core. The observed slight increase in the magnitude of the mixed alkali peak of the glass fiber after heat treatment (dashed curve in Fig. 12) was attributed to this increase in the number of dissimilar alkali pairs. The movement of the peak to slightly lower temperature is interpreted tentatively as a slight decrease in the mixed alkali peak activation energy.

Further evidence of the insensitivity of the mixed alkali peak to changes in the alkali ion distribution is provided by the observation (Taylor and Day<sup>(42)</sup>) that the mechanism responsible for the mixed alkali peak was unaffected by phase separation in silicate glasses.

On the other hand, the change in alkali distribution after heat treatment of the ion-exchanged glass at 590°C did decrease the magnitude of the alkali peak and shifted it to higher temperatures (Fig. 11). The change in the peak's position was interpreted tentatively as due to an increase in the activation energy of the alkali peak. The decrease in its magnitude is obviously caused by the further penetration of sodium ions into the glass decreasing the mobility of more lithium ions closer to the core of the glass fiber. The temperature shift is attributed to the corresponding increase in activation energy.

(Additional data given in Appendix C).

(H) Insensitivity of the Alkali Peak to Surface Compositions

Doremus' model<sup>(9)</sup> for internal friction predicts that the alkali damping peak should be sensitive to the composition of the sample's surface. The results depicted in Figures (6,7 and 8) can be used for examining this proposition. In Figure 6 for instance, the three fibers have the same concentration of lithium at the surface, but different alkali peak magnitudes, in contradiction to what would be expected from a mere surface effect. Also, the simultaneously ion-exchanged glass bar and fiber (see Fig. 8) should have the same surface lithium concentration; nevertheless the magnitude of the alkali peak is drastically

different in each case. It is concluded that the present experimental data are in conflict with the concept that the internal friction is entirely governed by the surface alkali ion concentration.

## VI. CONCLUSIONS

The mechanical damping of sodium ion exchanged  $\text{Li}_2\text{O}\cdot\text{Al}_2\text{O}_3\cdot 2\text{SiO}_2$  glass fibers is basically similar to that for conventionally melted mixed alkali aluminosilicate glasses. As sodium ions replace lithium ions, the original alkali peak becomes progressively smaller while a mixed alkali peak appears and becomes progressively larger.

In an ion-exchanged glass, the magnitude of the alkali peak and the mixed alkali peak is determined by the overall composition of the sample. This leads to the variation of the internal friction with the sample dimensions.

The alkali peak is mainly due to the stress induced diffusion of the lithium ions in the un-exchanged glass core plus some small contribution from the lithium ions at the single-mixed alkali interface. The change in alkali peak height can be used to calculate the penetration depth of the second alkali introduced by ion exchange methods.

The mixed alkali peak is associated with the mixed alkali surface layer and its magnitude is not sensitive to changes in alkali ion distribution as long as the total number of dissimilar alkali pairs is not changed. However, after attaining a uniform alkali distribution for an ion-exchanged glass, the alkali peak is reduced in magnitude.

The activation energy for both peaks in the ion-exchanged chilled glasses remains nearly constant. This indicates that the activation energy for the relaxation processes is primarily dependent upon the glass network structure. At 366°C, the ion exchange temperature, the network structure is unaffected by ion exchange, so the activation energy is not affected by the alkali ions present. Heat treatment of the ion-exchanged glass producing uniform alkali ion distribution results in a shift of the alkali peak to higher temperatures indicating an increase in its activation energy. As far as the mixed alkali peak is concerned, its activation energy is constant-or may be decreasing-after homogenizing the glass fiber.

Samples having the same alkali ion concentration at the surface exhibit alkali peaks of different magnitude. This indicates that surface composition does not predominantly or alone account for the internal friction of ion exchanged glasses.

Reheating the ion-exchanged glasses to a certain temperature was not found necessary for the mixed alkali peak mechanism to be operative.

## VII. REFERENCES

1. J.V. Fitzgerald, "Anelasticity of Glass: II," J. Amer. Ceram. Soc., 34 [11] 339-44 (1951).
2. L.C. Hoffman and W.A. Weyl, "Survey of Effect of Composition on Internal Friction of Glass," Glass Ind., 38 [2] 81-85 (1957).
3. E. Deeg, "Zusammenhang Zwischen Feinbau und mechanisch-akustischen Eigenschaften einfacher silikatgläser IV," (Relationship Between Structure and Mechanical-Acoustical Properties of Single Silicate Glasses: IV), Glastech. Ber., 31 [6] 229-40 (1958).
4. D.E. Day and Guy E. Rindone, "Properties of Soda Aluminosilicate Glasses: II, Internal Friction," J. Amer. Ceram. Soc., 45 [10] 496-504 (1962).
5. J.O. Isard, "The Mixed Alkali Effect in Glass," J. of Non-Crystalling Solids, 1, pp. 235-61 (1969).
6. K.E. Forry, "Two Peaks in Internal Friction as a Function of Temperature in Some Soda Silicate Glasses," J. Amer. Ceram. Soc., 40 [3] 90-94 (1957).
7. R. Jagdt, "Untersuchungen von Relaxationserscheinungen an Alkali-Silikat-Gläsern," (Studies of Relaxation

- Phenomena in Alkali Silicate Glasses), Glastech. Ber., 33 [1] 10-19 (1960).
8. G.L. McVay and D.E. Day, "Diffusion and Internal Friction in Single-Alkali Glasses," J. Amer. Ceramic Soc., 53 [5] 284-5 (1970).
  9. R.H. Doremus, "Delayed Elasticity in Ionic Conductors," J. Appl. Phys., 41 [8] 3366-71 (1970).
  10. R.J. Ryder and G.E. Rindone, "Internal Friction of Single Alkali Silicate Glasses Containing Alkaline-Earth Oxides: II," J. Am. Ceram. Soc., 44 [11] 532-40 (1961).
  11. M. Coenen, "Einfluss Der Anistropie auf Die Relaxation von Silikatgläsern und Allgemeine Systematik Der Dämpfungsamaxima in Gläsern," (Influence of anisotropy on the relaxation of silicate glasses and general systematics of damping maxima in glass). Physics of Non-Crystalline Solids, Proceedings of the International Conference, Delft, pp. 444-60, July 1964. Edited by J.A. Prins.
  12. R.H. Doremus, "Weathering and Internal Friction in Glass," J. of Non-Crystalling Solids, 3, pp. 369-74 (1970).

13. H. Rötger, "Über das elastische Relaxationsverhalten von einfachen und gemischten alkali-silikaten und von Borax," (Elastic Relaxation Behavior of Simple and Mixed Alkali Silicates and Borax), *Glastech. Ber.*, 31 [2] 54-60 (1958).
14. I. Mohyudding and R.W. Douglas, "Observations of the Anelasticity of Glasses," *Phys. Chem. Glasses*, 1 [3] 71-86 (1960).
15. D.E. Day and W.E. Steinkamp, "Mechanical Damping Spectrum for Mixed Alkali  $R_2O \cdot Al_2O_3 \cdot 6SiO_2$  Glasses," *J. Amer. Ceram. Soc.* 52 [11] 571-4 (1969).
16. J.E. Shelby, Jr., and D.E. Day, "Mechanical Relaxations in Mixed-Alkali Silicate Glasses: II," *J. Amer. Ceram. Soc.*, 53 [4] 182-87 (1970).
17. H. Rötger, "Elastische Nachwirkung durch Wärmediffusion (thermische Reibung) und Materiediffusion (eigentliche innere Reibung) bei periodischem und aperiodischem Vorgang," (Elastic After-Effects from Thermal Diffusion and Matter Diffusion by Periodic and Aperiodic Methods). *Glastech. Ber.*, 19 [6] 192-200 (1941).
18. W.E. Steinkamp, J.E. Shelby, and D.E. Day, "Internal Friction of Mixed-Alkali Silicate Glasses," *J. Amer. Ceram. Soc.*, 50 [5] 271 (1967).



19. G.L. McVay and D.E. Day, "Diffusion and Internal Friction in Na-Rb Silicate Glasses," J. Amer. Ceram. Soc., 53 [9] 508-13 (1970).
20. K. Horovitz, Z. Phys., 15, 369 (1923).
21. K. Horovitz, Z. Phys., 115, 424 (1925).
22. B.P. Nicol'sky, Zh. Fiz, Khim, 27, 724 (1953).
23. B.P. Nicol'sky and M.M. Schultz, Vest. leningr. gos. univ. (4), 73 (1963).
24. B.P. Nicol'sky, M.M. Schultz, A.A. Belyustin and A.A. Lev., "Glass Electrodes for Hydrogen and Other Cations, Principles and Practice," p. 174. Edited by G. Eisenman, Marcel Dekker, N.Y. (1967).
25. S.S. Kistler, "Stresses in Glass Produced by Non-Uniform Exchange of Monovalent Ions," J. Amer. Ceram. Soc., 45 [2] 59 (1962); also Research Corp. Brit. Pat. 917 388.
26. H. Garfinkel (Corning Co.) Belg. 618 740 (1962).
27. Pittsburgh Plate Br. 1 018 890, 1 027 136.
28. B.R. Karstetter and R.O. Voss, "Chemical Strengthening of Glass Ceramics in the System  $\text{Li}_2\text{O}\cdot\text{Al}_2\text{O}_3\cdot\text{SiO}_2$ ," J. Amer. Ceram. Soc., 50 [3] 133 (1967).

29. T.D. Taylor and G.E. Rindone, "Internal Friction of Ion-Exchanged Glasses," J. Amer. Ceram. Soc., 51 [5], 289-90 (1968); 53 [4] 227 (1970).
30. J.E. Shelby, Jr., "Mechanical Relaxation of Ion-Exchanged Alkali Silicate Glasses," J. Amer. Ceram. Soc., 53 [4] 226 (1970).
31. H. de Waal, "Internal Friction of Sodium Disilicate Glass after Ion Exchange," Phys. Chem. Glasses, 10 [3] 108-16 (1969).
32. H. de Waal, "On the Internal Friction in Ion-Exchanged Sodium Silicate Glasses and in Sodium Aluminoborate Glasses," Ph.D. Thesis, Delft Technical University, Delft, Holland (1967).
33. J.V. Fitzgerald, "Anelasticity of Glass: I, Introduction," J. Amer. Ceram. Soc., 34 [10] 314-19 (1951).
34. J.E. Shelby, Jr. and D.E. Day, "Mechanical Relaxations in Mixed Alkali Silicate Glasses: I, Results," J. Amer. Ceram. Soc., 52 [4] 169-174 (1969).
35. D.W. Moore, "Temperature Variation in Distribution of Relaxation Times in Aluminosilicate Glasses," To be published in Phys. and Chem. Glasses, June 1971; Ph.D. Thesis, Ceramics Eng. Dept., University of Missouri-Rolla.

36. Walter Slavin, *Atomic Absorption Spectroscopy*, Interscience Publishers, N.Y. (1968).
37. J.W. Robinson, "Determination of Sodium by Atomic Absorption Spectroscopy," *Anal. Chim. Acta.*, 23, 458-61 (1960).
38. R.H. Doremus, *Diffusion in Non-Crystalline Silicates*, p. 5 from *Modern Aspects of the Vitreous State*, V. 2, Edited by J.D. Mackenzie. Butterworths, London, (1962).
39. P.G. Shewman, *Diffusion in Solids*, p. 6, McGraw-Hill, N.Y. (1963).
40. T.D. Taylor, "Internal Friction of Ion Exchanged Alkali Silicate Glasses," Ph.D. Thesis, Ceramic Science, Penn. State University, (1971).
41. G.H. Frischat, "Elektrische Leitfähigkeit Ionenausgetauschter Gläser," (Electrical Conductivity of Ion-Exchanged Glasses), Proc. IX International Congress on Glass, Versailles, Sept. 27 - October 2, 1971; to be published.
42. S.W. Taylor and D.E. Day, "Internal Friction of Phase Separated Glasses," *Phys. Chem. Glasses*, 11 [4] 89-92 (1970).

VIII. APPENDICES

APPENDIX A  
Internal Friction Measurements

(A) Torsion Pendulum

Internal friction was determined from the decay of velocity of the oscillating pendulum. The velocity was measured by a light beam reflected from a mirror on the oscillating pendulum and focused on a silicon solar cell faced by two parallel slits. An electronic timer measured the time required for the light beam to travel between the two slits, as well as the period of oscillation of the pendulum. Because the time necessary for the light beam to travel the fixed distance between the slits is inversely proportional to the velocity, the internal friction was calculated using the equation:

$$Q^{-1} = \frac{1}{N\pi} \ln \left( \frac{t_n}{t_0} \right)$$

$$Q^{-1} = \text{internal friction}$$

$$N = \text{number of cycles}$$

$$t_n = \text{time required for the light beam to pass between the slits on the } n\text{th cycle}$$

$$t_0 = \text{time required for the light beam to pass between the slits on the zeroth cycle}$$

The inverted torsion pendulum apparatus is shown in Fig. 1.

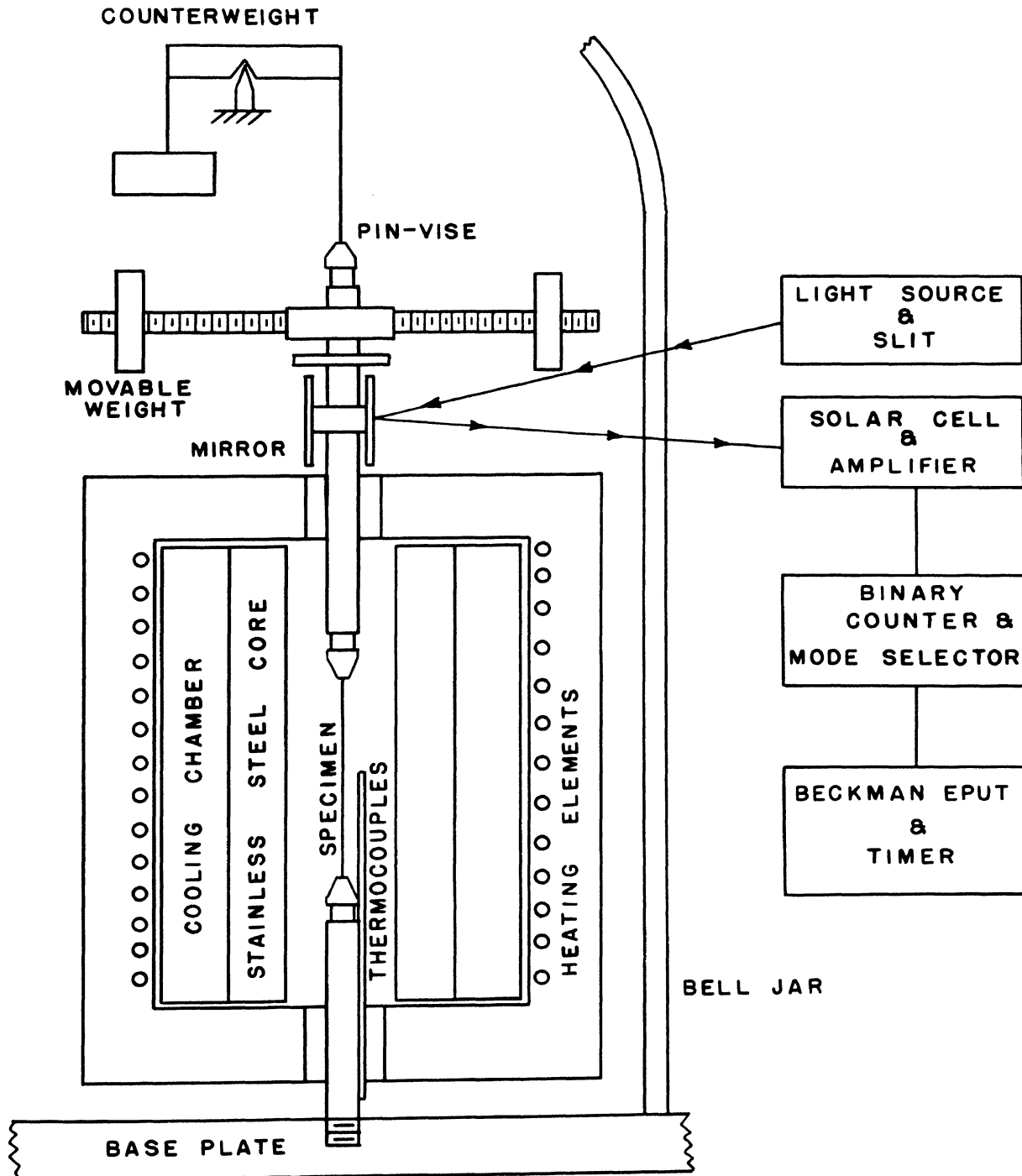


Fig. (1) Diagram of inverted torsion pendulum apparatus.

### (B) Resonance Technique

In this method the bar was suspended horizontally from two loops of fused silica thread located near the vibrational modes. The specimen was driven at its resonant frequency and allowed to decay, thus permitting the number of attenuated wave cycles occurring between known amplitude limits to be determined. Internal friction was calculated from the equation:

$$Q^{-1} = \frac{1}{N\pi} \ln \left( \frac{A_u}{A_L} \right)$$

where  $Q^{-1}$ ,  $N$ , and  $\pi$  are the same as defined under method A.  $A_u$  equals the upper amplitude limit and  $A_L$  the lower limit. The sonic apparatus is shown in Fig. 2.

In both methods A and B the apparatus was enclosed in a vacuum chamber operated at less than  $10^{-2}$  torr to eliminate air damping. The furnace was cooled below room temperature with liquid nitrogen. High temperatures were obtained using resistance windings on the outer surface of the coolant chamber.

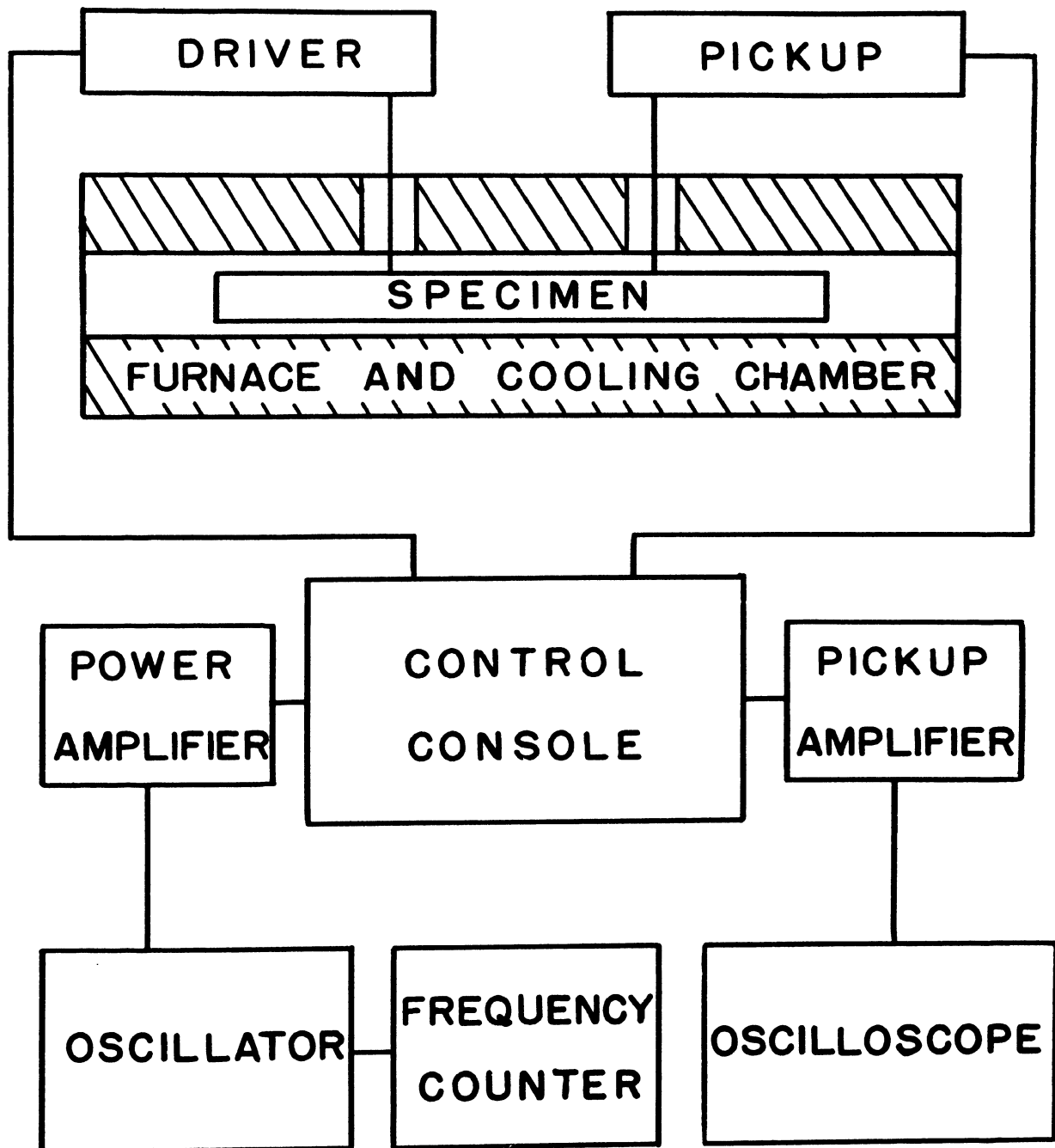


Fig. (2) Diagram of sonic apparatus



## APPENDIX B

## Atomic Absorption Spectrometry

In the atomic absorption system a light source, usually a hollow cathode lamp, supplies the sharp line spectra of the element under analysis (Na 5890 Å and for Li 6708 Å). The light source is chopped to eliminate any emission due to the flame. The solution containing the element under investigation is aspirated into the flame (air-acetylene oxidised flame of about 2300°C temperature) merely to dissociate it from its chemical bonds and place it into the unexcited ground state. The unexcited atoms strongly absorb the resonance spectral line from the lamp and the reduction in intensity is a function of concentration. The detection limits for Na is 0.002 µg/ml and that for Li is 0.0006 µg/ml. The sensitivity is about 0.015 µg/ml Na and 0.03 µg/ml Li for 1% absorption.<sup>(1)</sup>

The glass fibers were etched for one minute in a 5% HF acid solution (reagent grade) contained in Teflon beakers, then washed with distilled water and dried. After adding 1 ml 70% HNO<sub>3</sub> acid (reagent grade) to the HF solution it was evaporated to dryness. A potassium solution, HNO<sub>3</sub>, and distilled deionized water were added to measuring flask in order to achieve final concentration of 7% HNO<sub>3</sub> and 1000 µgK/ml. The same previous final concentrations was also used in the Na and Li standard solutions. The Na and Li

concentration profile were calculated by comparing the samples' absorption (which by proper dilutions was always in the linear region of the absorption vs. concentration) with absorption for the Na and Li standards. Sample solutions were stored in polyethylene bottles. It was always tried to avoid leaving the solutions in pyrex glass containers for long times to prevent them from dissolving some of the alkali from the pyrex container.

The Teflon beakers and polyethylene bottles were immersed for two days in dilute solutions of sodium tetraethylene diamine acetic acid to exchange any alkali or alkaline earths with the more soluble Na. Later the beakers, bottles, volumetric flasks, and other glassware were washed three times with 10% technical HCl solution and four times with distilled water to ensure eliminating any interferences as much as possible.

In analyzing the  $(1-x) \text{Li}_2\text{O} \cdot x \text{Na}_2\text{O} \cdot \text{Al}_2\text{O}_3 \cdot 2 \text{SiO}_2$  glass samples, it was necessary to insure that no other elements would interfere with the absorptions for the Na and Li ions.

Up to 3,000 p.p.m. K had no effect on Na absorption as indicated by Rubeska et al.<sup>(2)</sup> The determination of Na in silicate is generally interference-free.<sup>(3&4)</sup> David<sup>(5)</sup> reported no interference on 2 p.p.m. Na by 160 p.p.m. Al nor by 64 p.p.m. Si. Billings<sup>(6)</sup> found no molecular absorption on the Na line ( $5890 \text{ \AA}^{\circ}$ ) in an air-acetylene flame.

Robinson<sup>(7)</sup> found no ionization interference on 10 p.p.m. Na by 5,000 p.p.m. of K or Li.

As for lithium, Fishman and Downs<sup>(8)</sup> in an investigation of natural waters, found no interference on its (Li) determination by 1,000 p.p.m. Na, K or  $\text{NO}_3$ .

Slavin and Mulford<sup>(9)</sup> found no interference by Li on Si. Aluminum<sup>(9)</sup> interferes with alkaline earths, and not alkalis, by chemical combination.

## REFERENCES FOR APPENDIX B

1. "Analytical Methods for Atomic Absorption Spectrometry". Perkin-Elmer, Norwalk, Connecticut, Sept. 1968.
2. Rubeska, B. Moldan, and Z. Valniy, "The Determination of Sodium in Pure Limestones by Atomic Absorption Spectrophotometry," *Anal. Chim. Acta.* 29, 206-10 (1963).
3. G.K. Billings, "Major and Trace Element Relationships Within Coexisting Minerals of the Enchanted Rock Batholith," Llano Uplift, Texas, 74 pp., unpublished (1963).
4. G.K. Billings and J.A.S. Adams, "The Analysis of Geological Materials by Atomic Absorption Spectrometry," *Atomic Absorption Newsletter*, Perkin-Elmer Corp., 23, pp 1-7 (1964).
5. D.J. David, "The Determination of Exchangeable Na, K, Ca, & Mg in Soils by Atomic Absorption Spectrophotometry," *Analyst*, 85, pp. 495-503 (1960).
6. G.K. Billings, "Light Scattering in Trace Elements Analysis by Atomic Absorption," *Atomic Absorption Newsletter*, Perkin-Elmer Corp., 4, pp.357-61 (1965a).

- (7) J.W. Robinson, "Determination of Sodium by Atomic Absorption Spectroscopy," *Anal. Chem. Acta*, 23, pp. 458-61 (1960).
- (8) M.J. Fishman and S.C. Downs, "Methods for Analysis of Selected Metals in Water by Atomic Absorption," U.S. Geol. Survey, Water-Supply papers, 1540-c, 45 pp., U.S. Govt. Printing Office, Washington, (1966).
- (9) Atomic Absorption Spectrometry in Geology by Ernest E. Angino and Gale K. Billings, Elsevier Publishers, N.Y. (1967).

## APPENDIX C

Effect of Alkali Ion Distribution on the  
Internal Friction

Fig. 1 shows the internal friction of a chilled, ion exchanged fiber (15 minutes at  $366^{\circ}\text{C}$  in  $\text{NaNO}_3$ ) before and after heat treatment for three hours at  $590^{\circ}\text{C}$ . As mentioned previously and shown in Fig. 11, the height above background and position of the mixed alkali peak remained constant after homogenizing the fiber. Also, the alkali peak decreased in height and shifted to higher temperatures after the heat treatment. Although the period of ion exchange is the same for the fibers shown in Figures (11 and 1), the alkali peak before heat treatment is smaller in Fig. 11 compared to Fig. 1 because of the stabilization of the network structure.<sup>(1)</sup>

As concluded previously the mixed alkali peak is insensitive to the changes in alkali ion distribution. However, the alkali peak shifted to higher temperatures, indicating an increase in the activation energy, and decreased in magnitude due to the reduction of the  $\text{Li}^+$  ion mobility.

The change in the internal friction for the specimens in Fig. 1 is due to two factors: (1) the stabilization of the glass network and (2) the redistribution of the alkali ions.

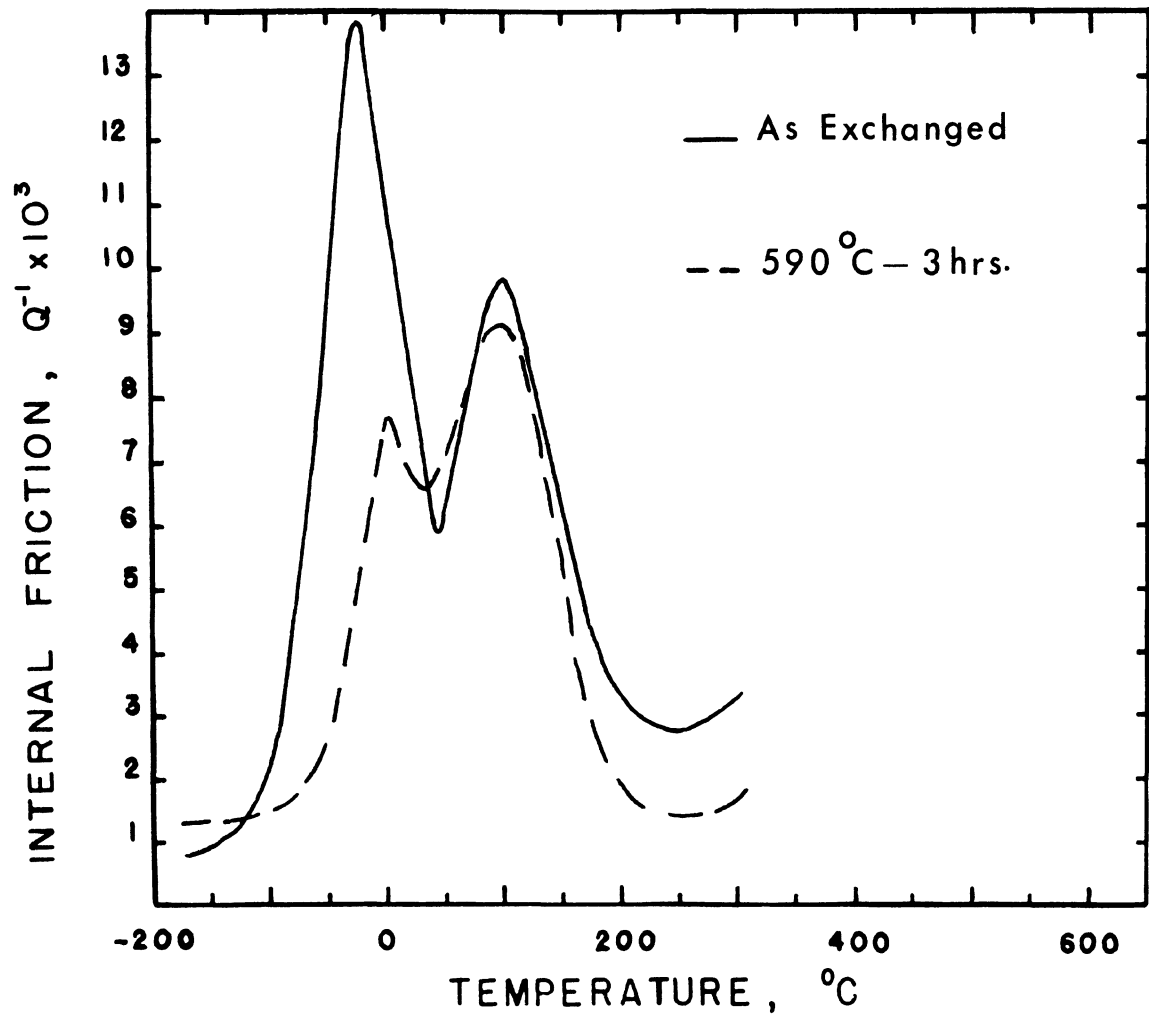


Fig. (1) Internal friction of sodium exchanged chilled  $\text{Li}_2\text{O}\cdot\text{Al}_2\text{O}_3\cdot 2\text{SiO}_2$  glass fibers (15 minutes in  $\text{NaNO}_3$  at  $366^\circ\text{C}$ ) having different alkali ion distribution due to heat treatment at  $590^\circ\text{C}$  for 3 hrs. ( $f = 0.7$  Hz).

## REFERENCES FOR APPENDIX C

1. G.J. Copley and D.R. Oaklay, "Internal Friction Studies of the Stabilization of Sheet Glass," *Phys. Chem. Glasses*, 9 [5] 141 (1968).



## APPENDIX D

Relation Between Alkali Peak Height and Penetration  
Depth of Introduced Second Alkali

The following material is the mathematical derivation of H. de Waal<sup>(1)</sup>. Internal friction can be determined from dissipation of energy of a specimen in forced torsional or flexural vibration. It is convenient to indicate the internal friction in terms of  $\frac{\Delta w}{w}$ , denoting the energy dissipated in a volume element per period divided by the total energy that entering the volume element during that period.  $\Delta w$ , the decrease of  $w$ , is the work done in one period on the volume element. The energy  $w$  is the maximum amount of work that has been done on the element of volume during one period. The work done during a time  $t$  can be written as:

$$A(t) = \int_0^t \tau \, d\gamma = \int_0^t \tau \, \dot{\gamma} \, dt \quad (1)$$

$\tau$  and  $\gamma$  are respectively the shear stress and shear strain on the volume element. For periodic vibration  $\tau$  and  $\gamma$  can be written

$$\tau = \tau_0 \sin \omega t \quad (2-a)$$

$$\gamma = \gamma_0 \sin(\omega t - \delta) \quad (2-b)$$

where  $\delta$  is the phase angle between  $\tau$  and  $\gamma$ .

Substitution of (2) into (1) gives:

$$A(t) = \tau_o \gamma_o \left\{ -\frac{1}{4} \cos(2\omega t - \delta) + \frac{1}{4} \cos(-\delta) + \frac{1}{2} \omega t \sin \delta \right\}$$

$A(t)$  reaches its maximum value for  $\omega t = \frac{\pi}{2} + \delta$

$$W = A_{\max} = \frac{1}{2} \tau_o \gamma_o \left\{ \cos \delta + \left( \frac{\pi}{2} + \delta \right) \sin \delta \right\} \quad (3)$$

To find  $\Delta w$  at time  $t$ , it must be recognized that  $A(t_1)$  consists of two parts, viz. the potential energy in the element of volume at the time  $t$ , and the dissipated energy between  $t = 0$  and  $t = t_1$ . The potential energy can be written, according to the theory of elasticity, as:

$$\begin{aligned} A_p(t_1) &= \frac{1}{2} \tau_1 \gamma_1 = \frac{1}{2} \tau_o \gamma_o \sin \omega t_1 \sin(\omega t_1 - \delta) \\ &= \tau_o \gamma_o \left\{ -\frac{1}{4} \cos(2\omega t - \delta) + \frac{1}{4} \cos(-\delta) \right\} \end{aligned}$$

Thus, the energy dissipated at the time  $t_1$  is:

$$A_D(t_1) = \frac{1}{2} \tau_o \gamma_o \cdot \omega t_1 \sin \delta$$

By taking  $t_1 = \frac{2\pi}{\omega}$ , the energy dissipated in one period becomes:

$$\Delta W = A_D \left( \frac{2\pi}{\omega} \right) = \pi \tau_o \gamma_o \sin \delta \quad (4)$$

$$\frac{\Delta W}{W} = \frac{\pi \tau_o \gamma_o \sin \delta}{\frac{1}{2} \tau_o \gamma_o \left\{ \cos \delta + \left( \frac{\pi}{2} + \delta \right) \sin \delta \right\}} = \frac{2\pi \sin \delta}{\cos \delta + \left( \frac{\pi}{2} + \delta \right) \sin \delta}$$

$$\frac{\Delta W}{W} \approx 2\pi \sin \delta \approx 2\pi \tan \delta \quad (\text{for small values of } \delta) \quad (5-a)$$

$$\text{or,} \quad \tan \delta = \frac{\Delta W}{2\pi W} \quad (5-b)$$

$\frac{\Delta W}{W}$  is the relative energy dissipation in one element of volume. Experimentally  $\frac{\Delta W^*}{W^*}$ , the dissipation of the specimen as a whole, is measured. Only under certain conditions may these quantities be interchanged. Assuming the principle of superposition to be valid we may write:

$$\frac{\Delta W^*}{W^*} = \frac{\int_{\text{vol}} \Delta W \, dv}{\int_{\text{vol}} W \, dv}, \quad (6)$$

when integrating over the volume of the specimen. In a torsion pendulum the stress varies throughout the specimen, which means that  $W$  is a function of volume,  $W = W(v)$ . In a torsion pendulum the vibration is a periodic function, so:

$$W^* = \int_{\text{vol}} W(v) \, dv$$

Thus,

$$\frac{\Delta W^*}{W^*} = \frac{\int_{\text{vol}} \left(\frac{\Delta W}{W}\right) \cdot W(v) \, dv}{\int_{\text{vol}} W(v) \, dv} \quad (7)$$

This expression shows  $\frac{\Delta W^*}{W^*} = \frac{\Delta W}{W}$  only if  $\frac{\Delta W}{W}$  is independent of the position in the specimen, i.e., the internal friction of the specimen must be amplitude independent and

that the specimen must be homogeneous.

Ion-exchanged fibers contain a concentration gradient of alkali ions. The surface layer, where the primary alkali ions have been partly replaced by another alkali, should be distinguished from the inner unaffected part of the fiber with the original composition.

The reduction in the height of the alkali peak can be calculated by assuming that the ion exchanged surface layer of the fiber no longer contributes to the alkali peak. To do this the relative contribution to the internal friction of each volume element in the fiber as a function of its position must be known.

Equation (7) relates  $(\frac{\Delta W^*}{W^*})$ , the energy dissipation of the entire specimen, with  $(\frac{\Delta W}{W})$ , the relative energy dissipation of an element of volume  $dv$ . Equation (5-b)

$\tan \phi = \frac{\Delta W}{2\pi W}$  is valid for each element of volume where  $\tan \phi$  is defined as the internal friction of the volume element.  $\phi$  is used, instead of  $\delta$ , to indicate that  $\tan \phi$  is not the experimentally measured internal friction. The measured internal friction can be written as:

$$\tan \delta = \frac{\Delta W^*}{2\pi W^*}$$

rewriting Equation (7):

$$\tan \delta = \frac{\int \tan \phi \cdot W(v) dv}{\int W(v) dv} \quad (8)$$

$\tan \phi$ , in ion exchanged fibers, is dependent upon the position of the volume element in the specimen so  $\tan \phi$  cannot be removed from the integral. When  $\delta$  is small Equation (3) may be replaced by:

$$W(v) = \frac{1}{2} \tau_0 \gamma_0 , \quad (9)$$

where  $\tau_0$  and  $\gamma_0$  are the maximum shear stress and strain, respectively. In a torsion experiment, stress and strain increase linearly with the distance  $r$  to the central axis of the fiber. From the theory of elasticity,  $\tau_0$  and  $\gamma_0$  are given by:

$$\tau_0 = \theta_0 G r \quad \text{and} \quad \gamma_0 = \theta_0 r , \quad (10)$$

where  $G$  represents the modulus of rigidity and  $\theta_0$  the maximum angular displacement of the fiber per unit of length. Substituting Equation (10) in Equation (9) gives:

$$W(v) = \frac{1}{2} G \theta_0^2 r^2$$

In combination with Equation (7):

$$\tan \delta = \frac{\int \tan \phi \cdot r^2 dv}{\int r^2 dv}$$

Assuming that  $G$  is a constant along the fiber radius:

$$v = \pi r^2 \ell$$

where  $\ell$  is fiber's length:

$$dv = 2\pi r \ell dr = (2\pi \ell) r dr$$

$$\begin{aligned} \tan \delta &= \frac{(2\pi \ell) \int_0^R \tan \phi r^3 dr}{(2\pi \ell) \int_0^R r^3 dr} = \frac{\int_0^R \tan \phi r^3 dr}{\int_0^R r^3 dr} \\ &= \frac{\int_0^R r^3 \tan \phi dr}{\left| \frac{r^4}{4} \right|_0^R} = \frac{4}{R^4} \int_0^R r^3 \tan \phi dr \end{aligned}$$

where  $R$  = radius of fiber,  $r$  = radius of union-exchanged core; from which it follows that:

$$R = r + \rho$$

where,  $\rho$  is depth of penetration of the second alkali, i.e., thickness of mixed alkali ion layer:

$$\tan \delta = \frac{4}{R^4} \left\{ \int_0^{R-\rho} r^3 \tan \phi dr + \int_{R-\rho}^R r^3 \tan \phi dr \right\}$$

If we assume that the alkali ions in the exchanged surface layer (of thickness  $\rho$ ) is not contributing to the alkali peak; then the right hand side of the in between brackets term of the last equation is zero.

Since the unexchanged core (its radius =  $r = R - \rho$ ) is a homogenous glass with the same concentration of lithium ions per unit volume throughout the fiber,  $\tan \phi$  is constant and could be removed from the integral:

$$\tan \delta = \frac{4}{R^4} \tan \phi \left\{ \frac{(R-\rho)^4}{4} \right\} = \tan \phi \left\{ \left( \frac{R-\rho}{R} \right)^4 \right\} = \tan \phi \left( \frac{r}{R} \right)^4$$

$$\left( \frac{\tan \delta}{\tan \phi} \right) = \left( \frac{r}{R} \right)^4 = \left( 1 - \frac{\rho}{R} \right)^4$$

which relates the reduction in height of alkali peak from its original value to the penetration depth of the replacing ions ( $\rho$ ).

## REFERENCES FOR APPENDIX D

1. H. de Waal, "On the Internal Friction in Ion Exchanged Sodium Silicate Glasses and in Sodium Alumino-borate Glasses," Ph.D. Thesis, Delft, Holland (1967)



## APPENDIX E

Internal Friction of Proton Exchanged  
 $\text{Li}_2\text{O}\cdot\text{Al}_2\text{O}_3\cdot 2\text{SiO}_2$  Glass

This appendix was submitted for publication in the  
Journal of the American Ceramic Society in August 1971.

## ABSTRACT

Protons were introduced into the surface of a  $\text{Li}_2\text{O}\cdot\text{Al}_2\text{O}_3\cdot 2\text{SiO}_2$  glass fiber (0.5 mm in diameter) by ion-exchange in  $\text{NH}_4\text{HSO}_4$  at  $366^\circ\text{C}$  for 21 hours. Infrared absorption measurements established that the protons were associated with bridging oxygen ions. After ion-exchange the magnitude of the alkali internal friction peak decreased while a new peak appeared at about  $220^\circ\text{C}$ . This new peak is attributed to the interaction of alkali and hydrogen ions, independent of the presence of nonbridging oxygen ions.

## I. INTRODUCTION

Single alkali glasses are characterized by two mechanical damping peaks. The peak occurring at lower temperatures has been related to the movement of the alkali ions<sup>(1-4)</sup> and is known as the alkali peak. The second peak occurring at higher temperatures has been attributed to several mechanisms<sup>(2,4-7)</sup>, one of which involves the stress induced movement of the non-bridging oxygen ions.<sup>(8,9)</sup> Glasses believed to contain only bridging oxygen ions, such as fused silica<sup>(10)</sup> and feldspar<sup>(9)</sup> glasses, do not exhibit this peak.

The dependence of the second internal friction peak upon OH content has raised questions whether this peak is due to non-bridging oxygen ions. In binary alkali silicate glasses this peak becomes larger with increasing OH content.<sup>(11,12)</sup> Coenen<sup>(11,13)</sup> associated this peak with the increasing concentration of bridging protons, as defined by Scholze<sup>(14)</sup>, and concluded it is due to an interaction between the alkali ions, bridging protons and oxygen ions. He also stated that a water-free sodium silicate glass did not exhibit this peak<sup>(11)</sup>, but published no experimental internal friction data for such a glass.

Doremus<sup>(15)</sup> recently related this peak to the weathering of glass and proposed that it is due to the stress induced

motion of hydrogen ions. Hydrogen ions are assumed to diffuse into the glass as the glass reacts with water vapor in the atmosphere.

The relative importance of the non-bridging oxygen ions to this peak is difficult to determine since most of the glasses studied contain both hydrogen (as OH groups) and non-bridging oxygen ions. The purpose of the present study was to determine whether hydrogen ions in a glass containing primarily bridging oxygen ions could produce an internal friction peak. By starting with a glass not showing this second peak, the effect of hydrogen on the internal friction would not be complicated by an existing peak.

## II. EXPERIMENTAL

A  $\text{Li}_2\text{O}\cdot\text{Al}_2\text{O}_3\cdot 2\text{SiO}_2$  glass was selected for study since it exhibits only one internal friction peak, alkali peak, and has a low background up to  $500^\circ\text{C}$ . Hydrogen was introduced into the glass by ion exchanging fibers (0.5 mm in diameter) in molten  $\text{NH}_4\text{HSO}_4$  (reagent grade) for 21 hrs at  $366^\circ\text{C}$ . After ion exchange, the fiber was washed with distilled water until the sulfate adhering to the surface had been removed. Internal friction was measured with an inverted torsion pendulum<sup>(16)</sup> operated at 0.65 Hz, in a vacuum ( $10^{-2}$  torr). Infrared absorption spectra were obtained on the same fiber used for the internal friction measurements, using a Beckman-IR5A Infrared spectrometer and hexachlorobutadiene as a solvent.

## III. RESULTS AND DISCUSSION

Fig. 1 shows the internal friction of the  $\text{Li}_2\text{O}\cdot\text{Al}_2\text{O}_3\cdot 2\text{SiO}_2$  glass before and after ion exchange in  $\text{NH}_4\text{HSO}_4$ . The alkali peak decreased in size and shifted to higher temperature ( $-30$  to  $-25^\circ\text{C}$ ) after ion exchange. A similar change in the alkali peak was observed by de Waal<sup>(17)</sup> for a sodium disilicate glass ion exchanged in  $\text{NH}_4\text{HSO}_4$  for 2 1/2 hrs at  $275^\circ\text{C}$ . Maklad and Kreidl<sup>(12)</sup> also reported a decrease in the size of the alkali peak in a sodium silicate glass (18 mole %  $\text{Na}_2\text{O}$ ) with increasing water content.

The ion exchanged glass clearly exhibits a second internal friction peak at  $220^\circ\text{C}$ . A second damping maximum is also observed in a Na ion-exchanged  $\text{Li}_2\text{O}\cdot\text{Al}_2\text{O}_3\cdot 2\text{SiO}_2$  glass.<sup>(16)</sup> Vaugin et al.<sup>(18)</sup> found a second peak at about  $+80^\circ\text{C}$  in a  $\text{Na}_2\text{O}\cdot 4\text{SiO}_2$  glass after exposure to the atmosphere for several days.

The infrared spectrum is shown in Fig. 2. Before ion exchange the only absorptions observed are those for hexachlorobutadiene (the doublet at  $6.3\text{-}6.5\ \mu\text{m}$ ). After ion exchange, additional absorptions are present at  $2.95$ ,  $3.45$  and  $4.45\ \mu\text{m}$ .

Several factors support an ion exchange between  $\text{Li}^+$  and  $\text{H}^+$  rather than between  $\text{Li}^+$  and  $\text{NH}_4^+$ . Fibers exchanged in  $\text{NH}_4\text{HSO}_4$  for more than 21 hours became increasingly fragile. This fragility is attributed to tensile stresses on the

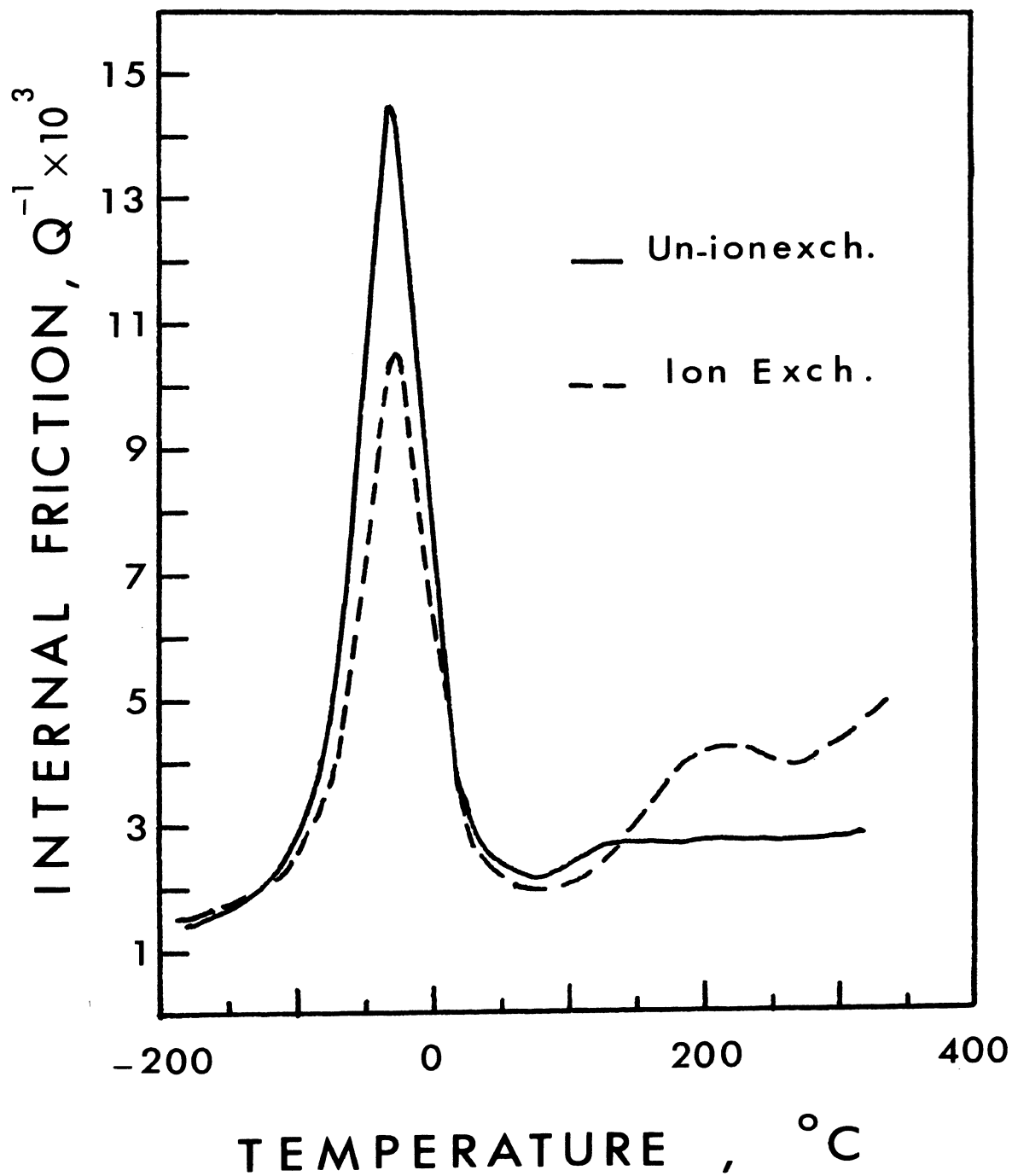


Fig. (1) Internal friction of a  $Li_2O \cdot Al_2O_3 \cdot 2SiO_2$  glass (chilled) before and after ion exchange in  $NH_4HSO_4$  at 366  $^{\circ}C$  for 21 hours. ( $f=0.63$  Hz).

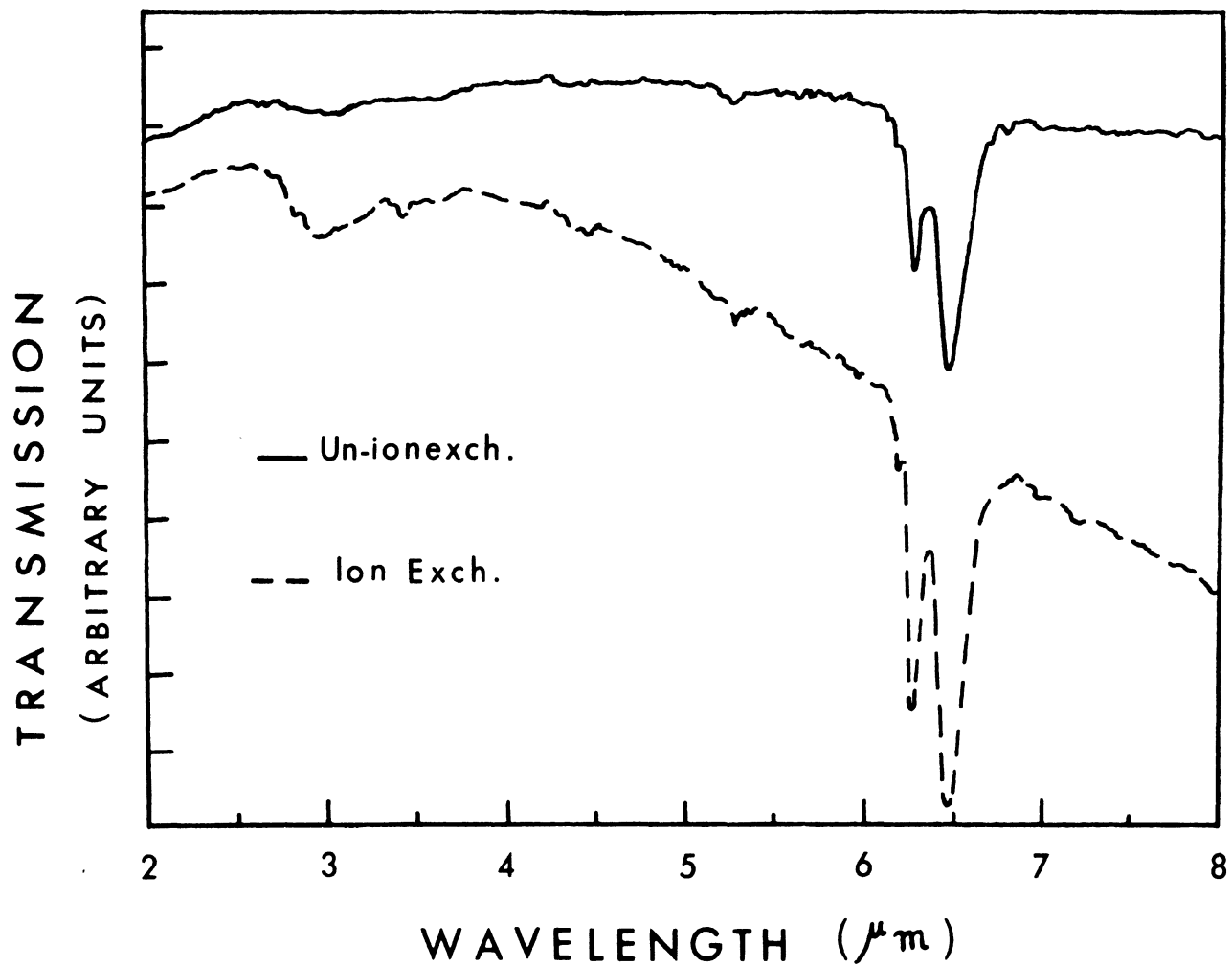


Fig. (2) Infrared transmission of the specimen used for internal friction measurements, Figure 1. Dashed curve was shifted (7%) for clarity.



surface of the fibers which developed as  $H^+$  replaced  $Li^+$ .  $NH_4^+$  would have produced compressive surface stresses which were not observed. Furthermore, the ion exchanged fibers showed a weight loss whereas the replacement of  $Li^+$  by  $NH_4^+$  would have produced a weight increase. An ion exchange between the alkali ions in a glass and the  $NH_4^+$  ions in  $NH_4HSO_4$  has been suggested<sup>(19)</sup>, but Ehrmann et al<sup>(20)</sup> showed the exchange was between  $H^+$  and the alkali ions.

Ideally, the structure of the original  $Li_2O \cdot Al_2O_3 \cdot 2SiO_2$  glass should consist of a continuous network with a minimum of non-bridging oxygen ions.<sup>(21-24)</sup> In interpreting the internal friction of the ion exchanged glass, therefore, it is important to consider whether the introduction of  $H^+$  changed the network structure. An interpretation of the infra-red spectrum for the ion exchanged glass, based on the assignments given by Scholze<sup>(14)</sup> to the absorptions caused by OH ions in silicate glasses, indicates that the network structure was unaffected by ion exchange.

Scholze<sup>(14)</sup> has shown that water in glass is characterized by three infrared absorption bands due to OH stretching vibrations. He identifies the absorption at 2.75 to 2.95  $\mu m$  with "a free-OH group," i.e., a hydrogen ion bonded to a bridging oxygen. The absorptions at 3.35 to 3.85  $\mu m$  and 4.25  $\mu m$  are assigned to hydrogen-bonded OH groups, with the former being assigned to OH groups associated by hydrogen bonding with non-bridging oxygen ions. The absorption at

4.25  $\mu\text{m}$  was assigned to structures containing several non-bridging oxygens and having the highest degree of hydrogen bonding.

According to Scholze, only the absorption at 2.75 to 2.95  $\mu\text{m}$  should be observed for protons in a glass that contains bridging oxygens only. The observed decrease in intensity of the 3.6  $\mu\text{m}$  absorption relative to that of the 2.8  $\mu\text{m}$  absorption with increasing  $\text{Al}_2\text{O}_3$  in  $20 \text{ Na}_2\text{O} \cdot X \text{ Al}_2\text{O}_3 \cdot (80-X) \text{ SiO}_2$  glasses, lead Scholze to conclude that non-bridging oxygen ions were essential for the 3.6  $\mu\text{m}$  absorption. This absorption disappeared completely when the Al/Na ratio equalled one, i.e. the glass contained only bridging oxygens.

The major difference between the infrared spectra shown in Fig. 2 is the absorption at 2.95  $\mu\text{m}$  in the ion exchanged glass. Since, two absorptions at 3.45 and 4.45  $\mu\text{m}$  are also barely perceptible, it is concluded that the ion exchanged glass is still essentially free of non-bridging oxygen ions. The infra-red spectrum for the ion exchanged glass is interpreted as indicating that the hydrogen ions are associated with bridging oxygens.

The present results are believed to show that hydrogen ions in a glass can produce an internal friction peak without the necessity for non-bridging oxygens being present. The second peak in the ion exchanged glass could be due to the movement of the hydrogen ions as suggested by Doremus. (15)

The proton penetration depth of the ion exchanged  $\text{Li}_2\text{O}\cdot\text{Al}_2\text{O}_3\cdot 2\text{SiO}_2$  glass was determined indirectly - by measuring the lithium concentration profile - to be about 25  $\mu\text{m}$ . Using de Waal's equation<sup>(25,16)</sup> for the decrease in the height of the alkali peak, the hydrogen ions were calculated to have penetrated about 20  $\mu\text{m}$  into the fiber. Doremus<sup>(15)</sup> estimated that a penetration depth of several hundred angstroms would be sufficient to cause an internal friction peak.

A second point to be considered, however, is that the changes in internal friction are similar when either  $\text{H}^+$  or  $\text{Na}^+$  are exchanged for  $\text{Li}^+$ . In both cases the alkali peak becomes smaller. As shown in Fig. 3, a second peak also appears at higher temperatures as  $\text{Li}^+$  ions are exchanged by  $\text{Na}^+$  ions. The second peak in the  $\text{Na}^+$  exchanged glasses has been identified<sup>(16)</sup> as being the same peak which is present in conventionally melted Li-Na Aluminosilicate glasses<sup>(26)</sup>, i.e., the mixed alkali peak. The mechanism proposed for the mixed alkali peak consists of a coupled reorientation of the dissimilar alkali ions.<sup>(27,28)</sup> This similarity in internal friction suggests, therefore, that the second peak at 220°C in the ion exchanged glass is a type of "mixed alkali peak" also, involving the cooperative movement of  $\text{Li}^+$  and  $\text{H}^+$  ions.

It is difficult to determine whether non-bridging oxygen ions are necessary for the second internal friction peak

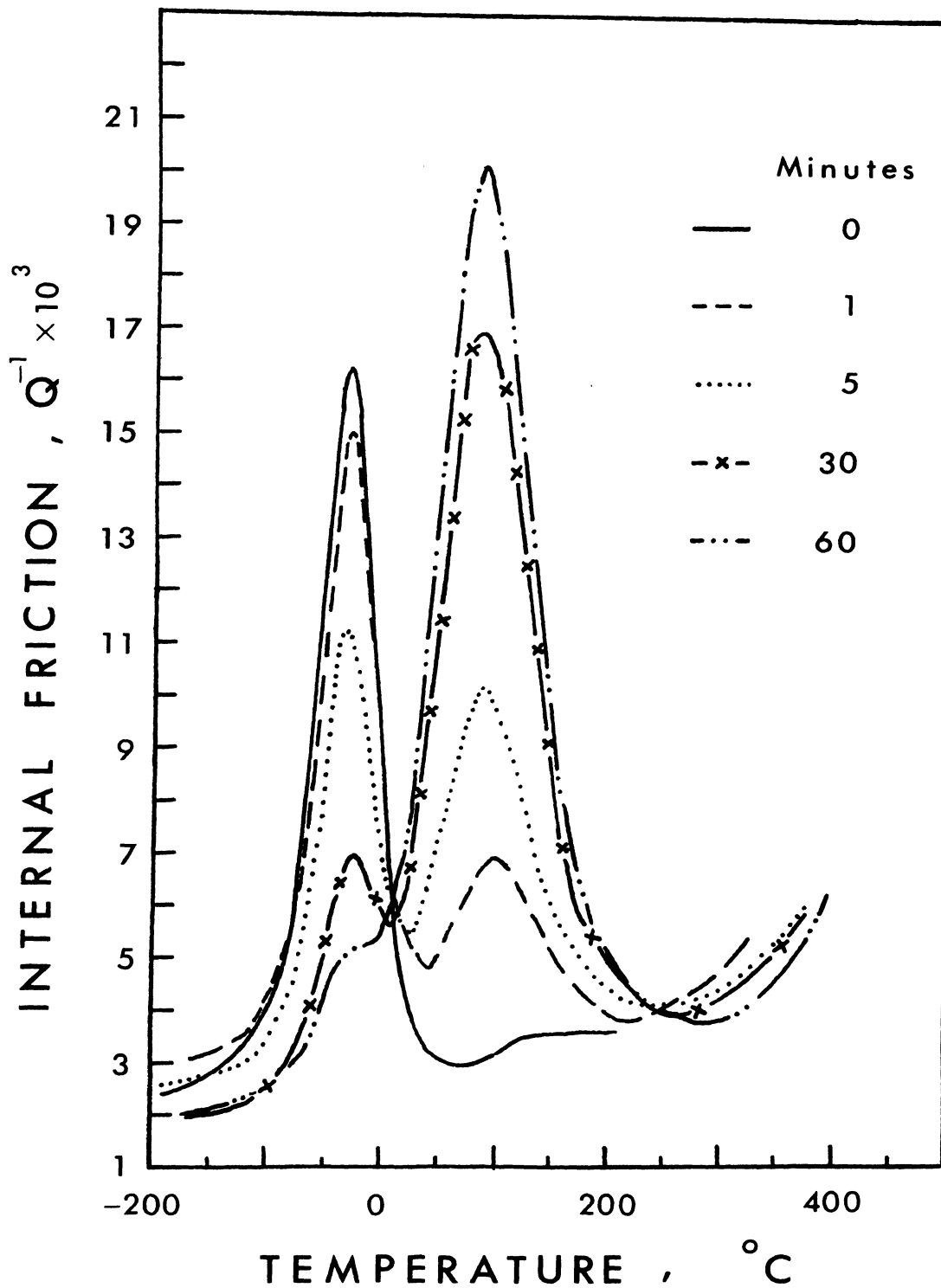


Fig. (3) Internal friction of a sodium exchanged  $\text{Li}_2\text{O} \cdot \text{Al}_2\text{O}_3 \cdot 2\text{SiO}_2$  glass fibers (chilled) after various periods of time in  $\text{NaNO}_3$  bath at  $366^\circ\text{C}$  ( $f = 0.5$  Hz; diameter =  $350 \pm 15 \mu\text{m}$ ).

(which has been called the non-bridging oxygen peak<sup>(8,9)</sup>) in alkali silicate glasses. Coenen<sup>(11)</sup> chose to attribute this peak to an interaction between the alkali, hydrogen and non-bridging oxygen ions. However, he was not aware that the mixed alkali peak is actually a new damping peak. Maklad and Kreidl<sup>(12)</sup> consider the peak due to the interaction of alkali and hydrogen but could not exclude the role of the non-bridging oxygen. It should be noted, however, that additions of a second alkali also gave the appearance that this peak was becoming larger<sup>(29)</sup> when instead the increase in magnitude was due to the appearance of a third peak, mixed alkali peak. Due to their proximity in temperature the two peaks were unresolved in certain mixed alkali glasses, e.g., Li-Na and Na-K. It is possible that the second peak in glasses containing non-bridging oxygen and hydrogen ions is the same as that observed in the H<sup>+</sup> ion exchanged glass or is composed of two unresolved peaks.

## IV. CONCLUSIONS

The exchange of  $H^+$  for  $Li^+$  ions in a  $Li_2O \cdot Al_2O_3 \cdot 2SiO_2$  glass produced changes in the internal friction similar to those observed when  $Na^+$  ions are ion-exchanged for  $Li^+$  ions. A second internal friction peak at  $220^\circ C$  in the ion-exchanged glass is attributed to the hydrogen ions, with the probable mechanism being the cooperative movement of lithium and hydrogen ions. Non-bridging oxygens are not a necessary precursor for the mechanism.

## REFERENCES FOR APPENDIX E

1. J.V. Fitzgerald, "Anelasticity of Glass: II," J. Amer. Ceram. Soc., 34 [11] 339-44 (1951).
2. L.C. Hoffman and W.A. Weyl, "Survey of Effect of Composition on Internal Friction of Glass," Glass Ind., 38 [2] 81-85 (1957).
3. E. Deeg, "Zusammenhang zwischen Feinbau und mechanisch-akustischen Eigenschaften einfacher silikatgläser IV," (Relationship Between Structure and Mechanical-Acoustical Properties of Single Silicate Glasses: IV), Glastechn. Ber., 31 [6] 229-40 (1958).
4. K.E. Forry, "Two Peaks in Internal Friction as a Function of Temperature in Some Soda Silicate Glasses," J. Amer. Ceram. Soc., 40, [3] 90-94 (1957).
5. R. Jagdt, "Untersuchungen von Relaxationserscheinungen an Alkali-Silikat-Gläsern," (Studies of Relaxation Phenomena in Alkali Silicate Glasses), Glastechn. Ber., 33 [1] 10-19 (1960).
6. J.V. Fitzgerald, K.M. Laing, G.S. Backman, "Temperature Variation of the Elastic Moduli of Glass," J. Soc. Glass Tech., 36 [169] 90-104T (1952); Ceramic Abst., 1952, Nov., p. 201C.

7. H. Rötger, "Über das elastische Relaxationsverhalten von einfachen und gemischten alkali-silikaten und von Borax," (Elastic Relaxation Behavior of Simple and Mixed Alkali Silicates and Borax), *Glastech. Ber.*, 31 [2] 54-60 (1958).
8. R.J. Ryder and G.E. Rindone, "Internal Friction of Single Alkali Silicate Glasses Containing Alkaline-Earth Oxides: II," *J.Amer.Ceram. Soc.*, 44 [11] 532-40 (1961).
9. D.E. Day and Guy E. Rindone, "Properties of Soda Aluminosilicate Glasses: II, Internal Friction," *J. Amer. Ceram. Soc.*, 45 [10] 496-504 (1962).
10. I. Mohyuddin and R.W. Douglas, "Observations of the Anelasticity of Glasses," *Phys. Chem. Glasses*, 1 [3] 71-86 (1960).
11. M. Coenen, "Einfluss Der Anistropie auf Die Relaxation von Silikatgläsern und Allgemeine Systematik Der Dämpfungsamaxima in Gläsern," (Influence of anisotropy on the relaxation of silicate glasses and general systematics of damping maxima in glass). *Physics of Non-Crystalline Solids, Proceedings of the International Conference, Delft*, pp. 444-60, July 1964. Edited by J.A. Prins.



12. M.S. Maklad and N.J. Kreidl, "Some Effects of OH Groups on Sodium Silicate Glasses," Proc. IX International Congress on Glass, Versailles, Sept. 27 - Oct. 2, 1971; to be published.
13. M. Coenen, "Mechanische Relaxation von Silikatgläsern eutektischer Zusammensetzung," (Mechanical Relaxation of Silicate Glasses with Eutectic Composition), Z. Elektrochem., 65 [10] 903-8 (1961).
14. Horst Scholze, "Der Einbau des Wassers in Gläsern," "Incorporation of Water in Glasses), Glastechn. Ber., 32 [3] 81-88; [4] 142-152; [7] 278-281; [8] 314-320 (1959).
15. R.H. Doremus, "Weathering and Internal Friction in Glass," J. of Non-Crystalline Solids, 3, pp. 369-74 (1970).
16. A. Ismail A. Abdel-latif and D.E. Day, "Internal Friction of Ion Exchanged  $\text{Li}_2\text{O} \cdot \text{Al}_2\text{O}_3 \cdot 2\text{SiO}_2$  Glasses," submitted for publication to the J. Amer. Ceram. Soc. (Aug. 1971).
17. H. de Waal, "Influence of Proton Exchange on Internal Friction in Alkali Silicate Glasses," J. Amer. Ceram. Soc., 52 [3] 165-6 (1969).

18. L. Vaugin, J.C. Braton, and P. Gobin, "Mesure du coefficient de frottement interieur de fines éprouvettes de Verre binaire  $\text{Na}_2\text{O}\cdot 4\text{SiO}_2$ ," (Measurement of Internal Friction of Fiber Samples in the Binary Glass  $\text{Na}_2\text{O}\cdot 4\text{SiO}_2$ ), *Verres et Refract.*, 23 [2] 174-80 (1969).
19. N.J. Kreidl, B.F. Trumm and R.F. Scott, "Electrolytical Replacement of Sodium by Ammonium in Glass," *J. Amer. Ceram. Soc.*, 24, pp. 225-8 (1941).
20. P. Ehrmann, M. de Billy and J. Zarzycki, "Etude de la migration 'ponctuelle' des ions hydrogène dans un verre à glace," (Punctuated Migration of Hydrogen Ions in a Plate Glass), *Verres et Refractaires*, 18 [3] 169-180 (1964); "Migration Des Ions  $\text{H}^+$  Dans Les Verres" (Migration of Hydrogen Ions in a Glass), 15 [2] 63-72 (1961); *ibid*, 15 [3] 131-139 (1961).
21. J.O. Isard, "Electrical Conduction in the Aluminosilicate Glasses," *J. Soc. Glass Technology*, 43, 113T (1959).
22. D.E. Day and G.E. Rindone, "Properties of Soda Aluminosilicate Glasses: III, Coordination of Aluminum Ions," *J. Amer. Ceram. Soc.* 45 [12] 579-81 (1962)

23. E.F. Riebling, "Structure of Sodium Aluminosilicate Melts Containing at Least 50 mole%  $\text{SiO}_2$  at  $1500^\circ\text{C}$ ," J. Chem. Phys. 44 [8] 2857-65 (1966).
24. E.D. Lacy, "Aluminum in Glasses and in Melts," Phys. Chem. Glasses, 4 [6] 234-38 (1963).
25. H. de Waal, "Internal Friction of Sodium Disilicate Glass after Ion Exchange," Phys. Chem. Glasses, 10 [3] 108-16 (1969).
26. D.E. Day and W.E. Steinkamp, "Mechanical Damping Spectrum for Mixed Alkali  $\text{R}_2\text{O}\cdot\text{Al}_2\text{O}_3\cdot 6\text{SiO}_2$  Glasses," J. Amer. Ceram. Soc. 52 [11] 571-4 (1969).
27. J.E. Shelby, Jr., and D.E. Day, "Mechanical Relaxations in Mixed-Alkali Silicate Glasses: II," J. Amer. Ceram., Soc., 53 [4] 182-87 (1970).
28. G.L. McVay and D.E. Day, "Diffusion and Internal Friction in Na-Rb Silicate Glasses," J. Amer. Ceram. Soc., 53 [9] 508-13 (1970).
29. J.E. Shelby, Jr., and D.E. Day, "Mechanical Relaxations in Mixed-Alkali Silicate Glasses: I, Results", J. Amer. Ceram. Soc., 52 [4] 169-74 (1969).

## IX. VITA

A. Ismail A. Abdel-Latif was born in Cairo, Egypt. He received his primary and secondary education in Cairo, Egypt; and a Bachelor of Science degree in Chemistry and Geology from Faculty of Science - Cairo University in May 1963.

Shortly after graduation he worked as a chemist and a head of a shift in Misr/Helwan spinning & weaving company, Cairo. In May 1964 he moved to the National Research Center, Metallurgy unit, where he worked as a research assistant until May 1969. At the same time, he was enrolled as a part-time graduate student in the American University, Cairo, from which he received his M.Sc. degree in Solid State Science in June 1968.

In July 7, 1969 he came over to U.S.A. From September 1969 until the present he attended graduate school, while receiving a Research Assistantship, at the University of Missouri-Rolla studying for a Ph.D. degree in Ceramic Engineering.

**202905**